Am J Transl Res 2015;7(5):781-803
www.ajtr.org /ISSN:1943-8141/AJTR0007352

Original Article

Adipose-derived mesenchymal stem cells embedded in platelet-rich fibrin scaffolds promote angiogenesis, preserve heart function, and reduce left ventricular remodeling in rat acute myocardial infarction

Yung-Lung Chen[1*], Cheuk-Kwan Sun[2*], Tzu-Hsien Tsai[1], Li-Teh Chang[3], Steve Leu[4], Yen-Yi Zhen[1], Jiunn-Jye Sheu[5], Sarah Chua[1], Kuo-Ho Yeh[1], Hung-I Lu[5], Hsueh-Wen Chang[6], Fan-Yen Lee[5†], Hon-Kan Yip[1,4,7,8†]

[1]Division of Cardiology, Department of Internal Medicine, Kaohsiung Chang Gung Memorial Hospital and Chang Gung University College of Medicine, Kaohsiung, 83301, Taiwan; [2]Department of Emergency Medicine, E-Da Hospital, I-Shou University School of Medicine for International Students, Kaohsiung, 82245, Taiwan; [3]Basic Science, Nursing Department, Meiho Institute of Technology, Pingtung, 91202, Taiwan; [4]Center for Translational Research in Biomedical Sciences, Kaohsiung Chang Gung Memorial Hospital and Chang Gung University College of Medicine, Kaohsiung, 83301, Taiwan; [5]Division of Thoracic and Cardiovascular Surgery, Department of Surgery, Kaohsiung Chang Gung Memorial Hospital and Chang Gung University College of Medicine, Kaohsiung, 83301, Taiwan; [6]Department of Biological Sciences, National Sun Yat-Sen University, Kaohsiung, 80424, Taiwan; [7]Center for Shockwave Medicine and Tissue Engineering, Kaohsiung Chang Gung Memorial Hospital and Chang Gung University College of Medicine, Kaohsiung, 83301, Taiwan; [8]Department of Medical Research, China Medical University Hospital, China Medical University, Taichung, 40402, Taiwan. [*]Equal contributors. [†]Equal contributors.

Received February 26, 2015; Accept April 11, 2015; Epub May 15, 2015; Published May 30, 2015

Abstract: *Objective:* This study tested the hypothesis that autologous adipose-derived mesenchymal stem cells (ADMSCs) embedded in platelet-rich fibrin (PRF) can significant promote myocardial regeneration and repair after acute myocardial infarction (AMI). *Summary background:* With avoiding the needle-related complications, PRF-embedded autologous ADMSCs graft provides a new effective stem cell-based therapeutic strategy for myocardial repair. *Methods:* Adult male Sprague-Dawley rats were equally divided (n = 8 per group) into group 1 (sham-operated), group 2 (AMI by ligating left coronary artery), group 3 (AMI+ PRF), and group 4 (AMI+PRF-embedded autologous ADMSCs). RPF with or without ADMSCs was patched on infarct area 1h after AMI induction. All animals were sacrificed on day 42 after echocardiography. *Results:* Left ventricular (LV) dimension and infarct/fibrotic areas were lowest in group 1, highest in group 2, in group 3 higher than in group 4, whereas LV performance and wall thickness exhibited a reversed pattern in all groups (all $p < 0.001$). Protein expressions of inflammatory (MMP-9, IL-1β), oxidative, apoptotic (Bax, cleaved PARP), fibrotic (Smad 3, TFG-β), hypertrophic (β-MHC), and heart failure (BNP) biomarkers displayed an identical pattern in infarct/fibrotic areas, whereas the protein expressions of anti-inflammatory (IL-10), anti-apoptotic (Bcl-2), anti-fibrotic (Smad1/5, BMP-2) biomarkers and α-MHC showed an opposite pattern (all $p < 0.01$). Angiogenic activities (c-Kit+, Sca-1+, CD31+, SDF-1α+, CXCR4+ cells; protein expressions of SDF-1α, CXCR4, VEGF) were highest in group 4 and lowest in group 1 (all $p < 0.001$). *Conclusion:* ADMSCs embedded in PRF offered significant benefit in preserving LV function and limiting LV remodeling after AMI.

Keywords: Acute myocardial infarction, engineered tissue, platelet-rich fibrin, mesenchymal stem cells

Introduction

Acute myocardial infarction (AMI) is the leading cause of death in patients hospitalized for cardiovascular disease [1]. Left ventricular (LV) remodeling following AMI, which eventually leads to LV dilatation and pump failure, independently accounts for poor clinical outcomes [2-4]. Although early successful reperfusion using thrombolytic therapy or primary percutaneous coronary intervention is the most effective therapeutic measures taken to minimize the ischemic insult and infarct size of the myocardium and ultimately improve the overall clini-

cal outcome [5-7], loss of myocardium after AMI is always irreversible. One of distinct importance is that the severity of pump failure is typically associated with infarct size and ischemic area [2-4, 8, 9]. Thus, restoring lost myocardium, i.e., repair/regeneration of functional myocardium, is the ultimate goal of cardiac tissue engineering.

Growing evidence from both animal model studies and clinical trials has shown promising treatment outcomes using mesenchymal stem cell (MSC) or endothelial progenitor cell (EPC) in various settings of diseases, including ischemic heart disease, in particular, AMI [10-14]. Indeed, a number of previous studies have demonstrated the therapeutic potential of cell treatment against a myriad of organ dysfunction regardless of whether the etiologies are ischemia-related [10-16].

Interestingly, the most common method for cell implantation in experimental studies is direct myocardial needle injection of cell suspensions [10, 13, 16]. Albeit simple, this method is associated with several pitfalls such as rapid cell loss from leakage through the injection site, needle-mediated direct tissue damage, or even heart perforation with uncontrollable hemorrhage due to infarct-related thinning and fibrosis of LV wall. It is, therefore, clear that the clinical applicability of this approach is limited. Accordingly, an alternative strategy for cell administration should be developed not only to avoid the needle-related complications, but also to ensure more secure contact between the ischemic myocardium and the introduced cells to augment the therapeutic outcome. Recently, biological scaffolding with tissue engineering has been suggested to be a new strategy for effective delivery of stem cells for myocardial repair [17, 18]. Application of this technique, i.e., "patching" for myocardial repair using different engineered materials such as autologous MSC/EPC grafts in the setting of AMI, may, therefore, improve LV function and limit LV remodeling by at least two mechanisms: 1) myocardial regeneration from enhanced angiogenesis, paracrine effects, and possible myocardial differentiation from MSCs/EPCs, and 2) mechanical support, i.e., ventriculoplasty to reduce chamber size and, therefore, the wall stress. Additionally, studies have recently shown that adipose tissue is a promising source of autologous stem cells (i.e., adipose-derived mesenchymal stem cell, ADMSC) for the treatment of ischemia-related organ dysfunction [19, 20]. Therefore, this study, by using a rodent AMI model, attempted to test the hypothesis that: 1) The scaffold made from platelet-rich fibrin (PRF), when patched on the infarct area, might preserve LV function and inhibit LV remodeling; 2) Introduction of ADMSCs into PRF, i.e., "autologous ADMSC graft", may be superior to the RPF scaffold alone in improving LV function and limiting LV remodeling.

Materials and methods

Ethics

All animal experimental procedures were approved by the Institute of Animal Care and Use Committee at Chang Gung Memorial Hospital-Kaohsiung Medical Center (Affidavit of Approval of Animal Use Protocol No. 2010122405) and performed in accordance with the Guide for the Care and Use of Laboratory Animals (NIH publication No. 85-23, National Academy Press, Washington, DC, USA, revised 1996).

Animal grouping and isolation of adipose tissue for culture of adipose-derived mesenchymal stem cells

Pathogen-free, adult male Sprague-Dawley (SD) rats (n = 32) weighing 320-350 g (Charles River Technology, BioLASCO Taiwan Co. Ltd., Taiwan) were randomized and equally divided into group 1 (sham controls receiving thoracotomy only, n = 8), group 2 (AMI induction only, through left coronary artery ligation, n = 8), group 3 (AMI + PRF scaffold, n = 8), and group 4 (AMI + ADMSC-embedded PRF scaffold, n = 8). The dosage of ADMSC (2.0×10^6) was chosen according to our previous study with minor modifications [13, 16].

Rats in group 4 was anesthetized with inhalational 2% isoflurane 14 days before AMI induction for harvesting peri-epididymal adipose tissue, as we previously reported [19, 20]. Isolated ADMSCs were cultured in a 100 mm diameter dish with 10 mL DMEM culture medium containing 10% FBS for 14 days. Flow cytometric analysis was performed to identify cellular characteristics after cell-labeling with appropriate antibodies on day 14 of cell cultivation prior to implantation (**Figure 1**).

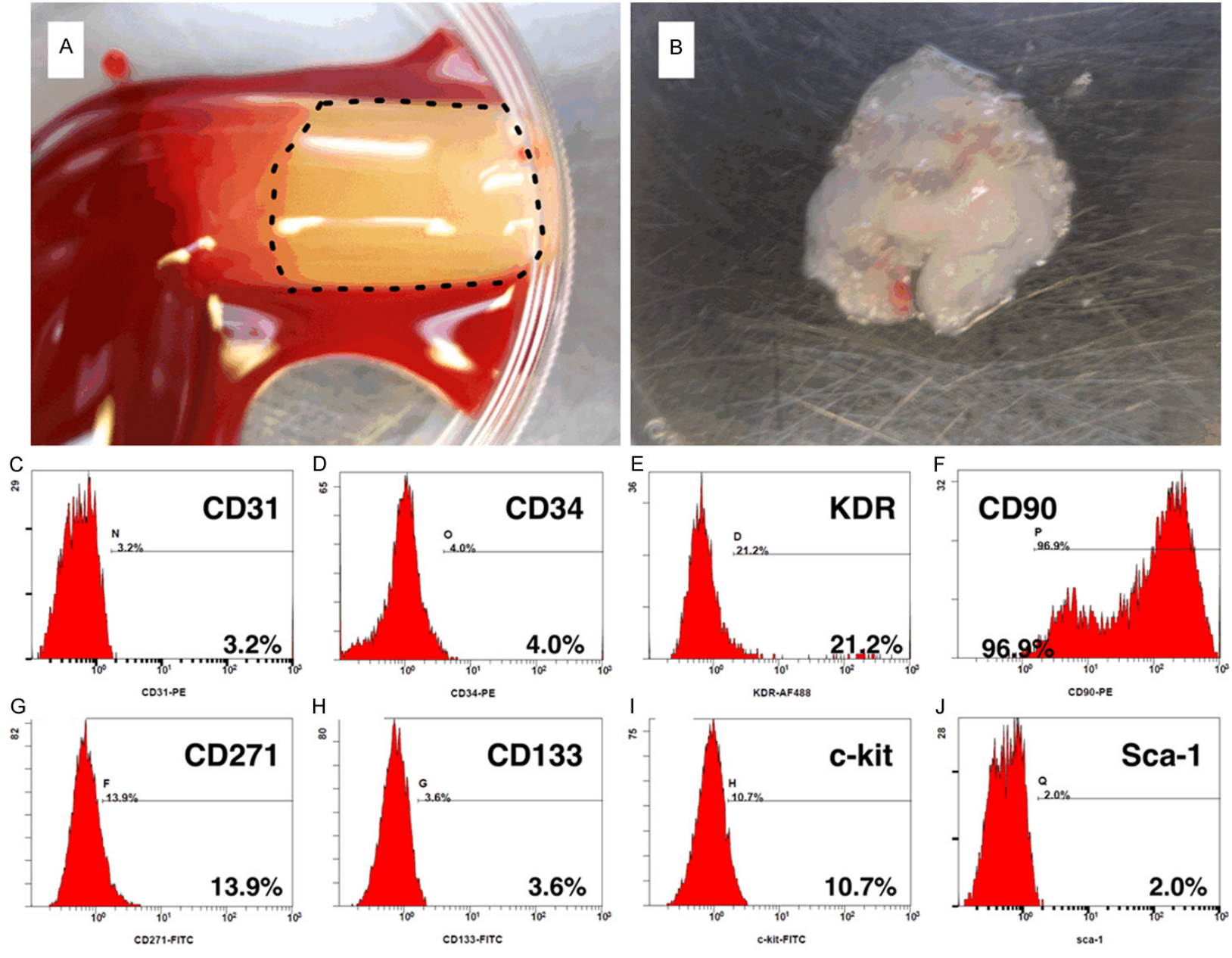
A
B
C
CD31
N
3.2%
3.2%
CD31-PE
D
CD34
O
4.0%
4.0%
CD34-PE
E
KDR
D
21.2%
21.2%
KDR-AF488
F
CD90
P
96.9%
96.9%
CD90-PE
G
CD271
F
13.9%
13.9%
CD271-FITC
H
CD133
G
3.6%
3.6%
CD133-FITC
I
c-kit
H
10.7%
10.7%
c-kit-FITC
J
Sca-1
Q
2.0%
2.0%
sca-1

K

Markers	CD31	CD34	KDR	CD90	CD271	CD133	c-kit	Sca-1
%	5.24 ± 3.47	3.73 ± 1.66	18.31 ± 6.21	81.24 ± 9.62	4.85 ± 4.90	4.44 ± 3.37	12.63 ± 7.59	2.30 ± 1.67

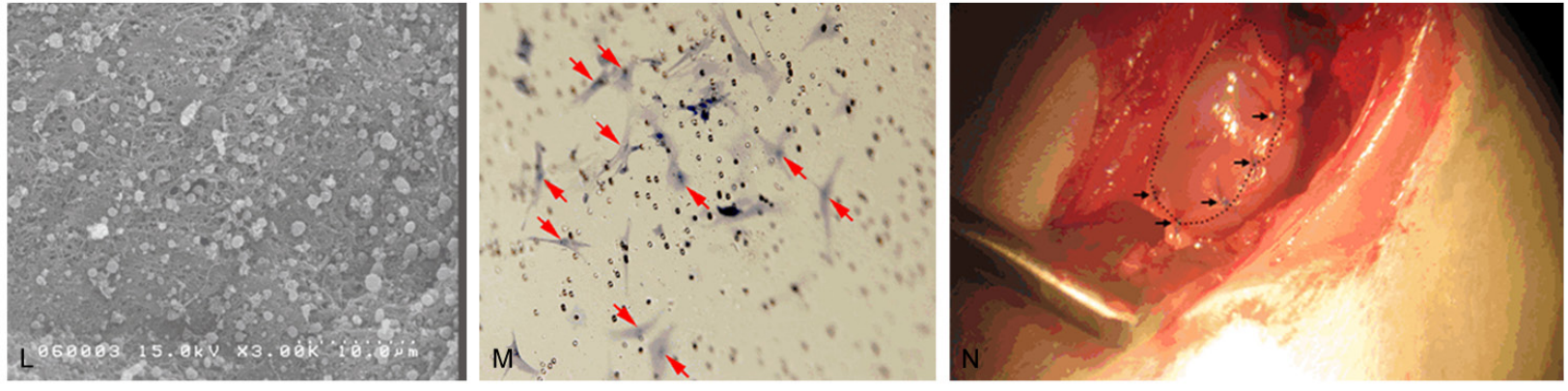

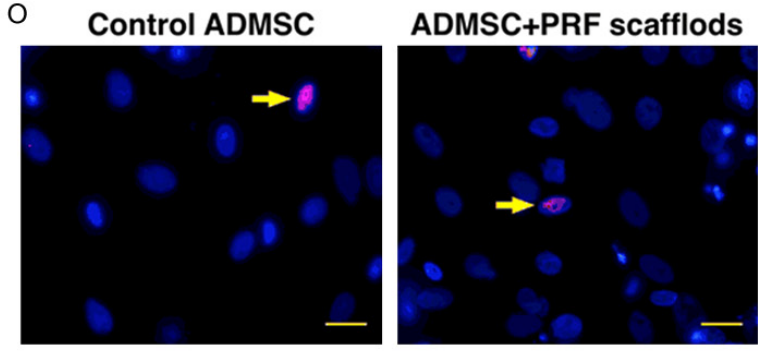

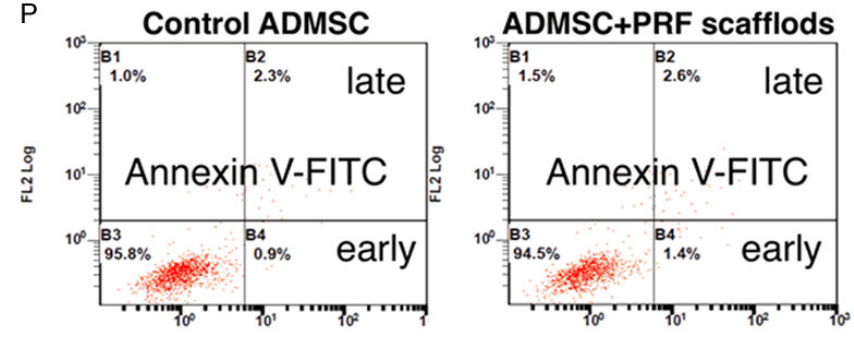

Variables	Control ADMSC	ADMSC + PRF Scaffolds	p-value
γ- H2AX (%)	0.83 ± 0.75	1.17 ± 0.74	0.473

Variables	Control ADMSC	ADMSC + PRF Scaffolds	p-value
Early apoptotic cells	2.2 ± 0.1	2.3 ± 0.2	0.894
Late apoptotic cells	0.8 ± 0.1	1.2 ± 0.1	0.217

Figure 1. Preparation of platelet-rich fibrin (PRF) scaffold and engineered adipose-derived mesenchymal stem cell (ADMSC) grafts and flow cytometric analysis of stem cells at day 14 cell culturing. A. The PRF scaffold, white jelly-like component, (black dot-line square) was already prepared in the Eppendorff tube. B. The example of one piece of engineered ADMSC grafts had been prepare and already for patching on the infarct area. C to J. The illustration of flow cytometric expressions

of endothelial progenitor cells (EPCs) and ADMSCs at day-14 cell culture in DMEM culture medium. K. The mean distributions (n = 6) of EPC (CD31, CD34, KDR, CD133) and ADMSC (CD90, CD271, Sca-1, c-Kit) surface markers. CD90 (i.e., ADMSC) was the highest population among the culturing stem cells. L. The scanning electronic microscopy clearly identified the morphological feature of the homogeneous and network-like PRF scaffold with the attachment of numerous ADMSCs (black arrows) in the surface layer of the scaffold. M. Under microscopic finding (100 ×), numerous DAPI stained ADMSCs (red arrows) were identified at the bottom layer of the transwell membrane after 24 h migration. N. Illustrating the PRF scaffold (black dotted line) which was covered on the surface of infarct area and was sutured (black arrows) for fixation. O. The immunofluorescent microscopic findings (400 ×) showed no difference in γ-H2AX+ cells (yellow arrows) between with and without PRF scaffold treatment. Scale bars in right lower corners represent 20 μm. P. The flow cytomtric analysis displayed no difference in early or late apoptosis of ADMSC between with and without PRF scaffold treatment.

Preparation of PRF, ADMSC labeling, and AMI induction

On day 14, CM-DiI (Vybrant™ DiI cell-labeling solution, Molecular Probes, Inc.) (50 μg/mL) and XenoLight DiR (a near-infrared fluorescent cyanine dye, Caliper Life Science) were added to the culture medium 30 minutes before AMI induction for ADMSC (1.0×10^6 cells per batch) labeling as previously reported [20]. At the same time, 3.0 mL of blood was drawn through cardiac puncture from a donor rat and placed in an Eppendorff tube, followed by centrifugation (model 5415D; Eppendorf) at 400g for 10 minutes at room temperature. The suspension of white jelly-like component, so-called "PRF scaffold", was collected after centrifugation (**Figure 1**). The PRF scaffold was then cut into two pieces each of which was placed at the bottom of an Eppendorff tube. Two batches of ADMSCs (1.0×10^6 each) previously labeled with CM-DiI and XenoLight DiR were pipetted onto the two pieces of PRF in the Eppendorff tubes, respectively, before being centrifuged at 800 xg for 20 minutes. This procedure helped in the embedment of ADMSCs into the PRF scaffold. The ADMSC-embedded PRF scaffolds were referred to as "engineered ADMSC grafts".

To elucidate the morphology and the pore size of the PRF scaffold, the scanning electron microscopy (SEM) was performed (**Figure 1L**) after the PRF scaffold were well prepared. Additionally, in order to make sure that the engineered ADMSCs could passed through PRF Scaffold and migrated into the myocardium, the ADMSCs were put into the upper layer of the transwell for 24 h for migration and the membrane of the transwell was then removed for identification of the ADMSCs at the bottom layer of the membrane (**Figure 1M**).

To determine whether PRF scaffold was toxic to ADMSCs the immune fluorescent stain for identification of γ-H2AX, and indicator of DNA damage, was performed (**Figure 1O**). Additionally the percentages of viable and apoptotic ADMSCs were determined by flow cytometry using double staining of annexin V and propidium iodide (PI); this is a simple and popular method for the identification of apoptotic cells (i.e. early [annexin V+/PI-] and late [annexin V+/PI+] phases of apoptosis) (**Figure 1P**).

During the preparation of PRF scaffold and engineered ADMSC grafts, all animals were anesthetized by inhalational 2.0% isoflurane and placed in a supine position on a warming pad at 37°C. Under sterile conditions, the heart was exposed via a left thoracotomy. Acute myocardial infarction was induced in group 2 to 4 animals by left coronary artery ligation 3 mm distal to the margin of left atrium with 7-0 prolene suture. Regional myocardial ischemia was verified by observing a rapid color change from pinkish to dull reddish over the anterior surface of the LV and rapid development of akinesia and dilatation in the at-risk region. Rats receiving thoracotomy only without AMI induction served as sham controls (group 1).

The well-prepared PRF scaffolds and engineered ADMSC grafts in groups 3 and 4, respectively, were patched on the hearts with the upper surface of the patches in the Eppendorff tubes being placed in direct contact with the heart surface and sutured in place. After the procedure, the thoracotomy wound was closed and the animals were allowed to recover from anaesthesia in a portable animal intensive care unit (ThermoCare®) for 24 hours.

Functional assessment by echocardiography

All animals underwent transthoracic echocardiography under general anesthesia in supine position at the beginning and end of the study.

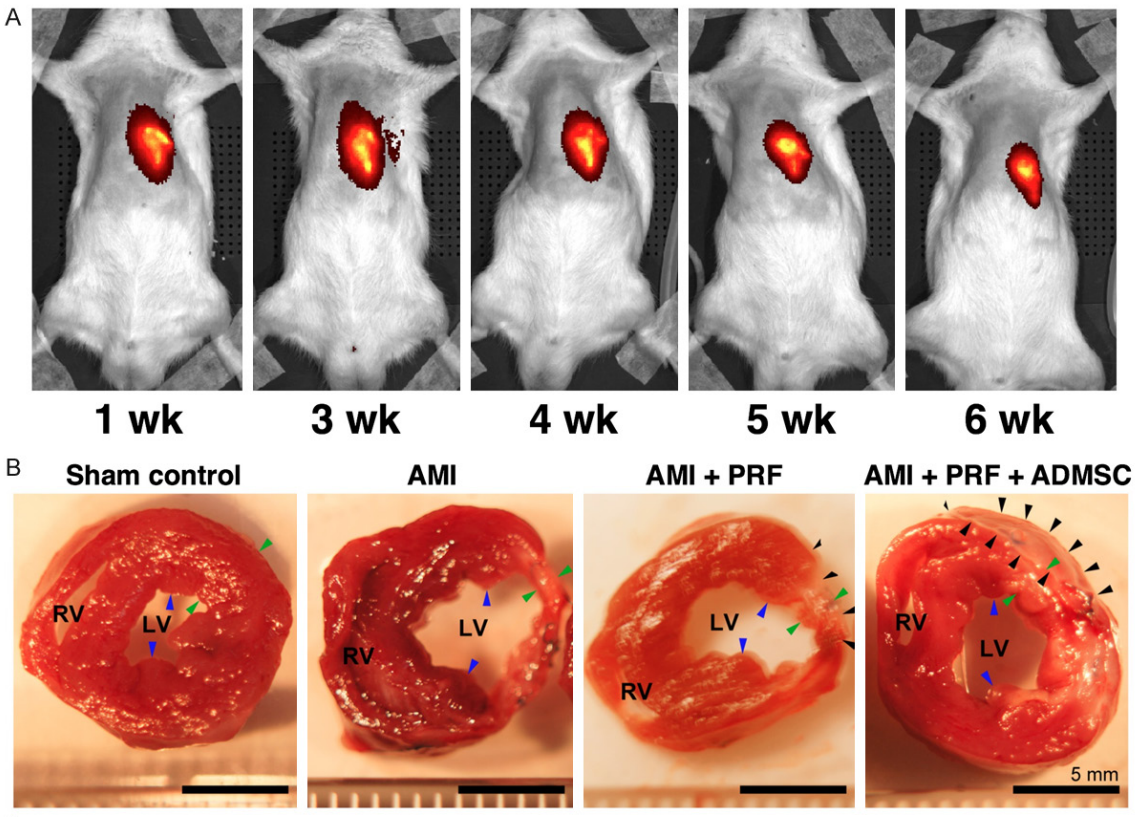

C

Group	Sham control	AMI	AMI+PRF	AMI+PRF +ADMSC	*p* value
Wall thickness (mm)	3.82 ± 0.34*	1.31 ± 0.36†	1.72 ± 0.32‡	2.92 ± 0.70§	<0.001

Figure 2. Illustration of IVIS study and anatomical and pathological findings on day 42 after AMI induction (n = 8). A. Serial assessments of living imaging by *In Vivo* Imaging System (IVIS) after acute myocardial infarction (AMI). B. The anatomical findings showed the cross-section area of the heart at the papillary muscle (blue arrows) among the four groups. The left ventricular (LV) chamber size was highest in AMI group, lowest in sham-control group, and notably higher in AMI + platelet-rich fibrin (PRF) group than in AMI + PRF + adipose-derived mesenchymal stem cell (ADMSC); Conversely, the infarct size showed an apposite pattern of LV chamber size. The black arrows indicated PRF scaffold tissue in AMI + PRF group and ADMSC-embedded PRF scaffold (AMI + PRF + ADMSC) (i.e., engineered ADMSC grafts) group, respectively. Scale bars in right lower corners represent 5 mm. C. *vs. other groups with different symbols (*, †, ‡, §), $p < 0.001$. Statistical analysis using one-way ANOVA, followed by Bonferroni multiple comparison post hoc test. Symbols (*, †, ‡, §) indicate significance (at 0.05 level).

The procedure was performed by an animal cardiologist blind to the experimental design using an ultrasound machine (Vevo 2100, Visualsonics). M-*mode* standard *two-dimensional* (2D) left parasternal-*long axis* echocardiographic examination was conducted. Left ventricular internal dimensions [end-systolic diameter (ESD) and end-diastolic diameter (EDD)] were measured according to the American Society of Echocardiography leading-edge method using at least three consecutive cardiac cycles. LVEF was calculated as follows: LVEF (%) = [($LVEDD^3$-$LVEDS^3$)/$LVEDD^3$] × 100%.

Serial IVIS examination after AMI for 6 weeks

Additionally, for tracing the ADMSCs embedded in the "engineered ADMSC grafts" on the infarcted LV myocardium, *in vivo* imaging studies using IVIS (Xenogen IVIS 200) was serially performed weekly up to the end of 6 weeks after AMI induction with the ADMSCs being pre-

labeled with a XenoLight DiR (**Figure 2A**) in the animals.

Sample collection for individual study and measurement of wall thickness in infarct area at papillary muscle level

By the end of the study period (i.e., 6 weeks after AMI induction) when the last echocardiographic measurements were finished, the rats were euthanized with the hearts harvested. For each animal, the whole heart weight, weight of left ventricle + septum, and body weight were recorded from which the ratio of total heart weight to final body weight was calculated. In addition, to determine the wall thickness in the infarct area, the heart in each rat was cut into two pieces at the middle level of left ventricle (i.e., at papillary muscle level) and a photo of the cross section was taken at fixed distance (**Figure 2B**). The LV infarct region was then cut into pieces, some of which were fixed with OCT (Tissue-Tek) for immunohistochemical (IHC)/immunofluorescent (IF) staining. Other pieces were either fixed in 4% paraformaldehyde/0.1% glutaradehyde PBS solution before being embedded in paraffin blocks for hematoxylin-eosin staining or stored at -80°C for protein analyses.

Western blot analysis of heart tissue

Equal amounts (50 μg) of protein extracts were loaded and separated by SDS-PAGE using acrylamide gradients. After electrophoresis, the separated proteins were transferred electrophoretically to a polyvinylidene difluoride (PVDF) membrane (Amersham Biosciences). Nonspecific sites were blocked by incubation of the membrane in blocking buffer [5% nonfat dry milk in T-TBS (TBS containing 0.05% Tween 20)] overnight. The membranes were incubated with the indicated primary antibodies [Bax (1:1000, Abcam), cleaved poly (ADP-ribose) polymerase (PARP) (1:1000, Cell Signaling), Bcl-2 (1:200, Abcam), phosphorylated (p)-Smad3 (1:1000, Cell Signaling), p-Smad1/5 (1:1000, Cell Signaling), bone morphogenetic protein (BMP) 2 (1:5000, Abcam) transforming growth factor (TGF)-β (1:500, Abcam), interleukin (IL)-1β (1:1000, Cell Signaling), matrix metalloproteinase (MMP)-9 (1:3000, Abcam), IL-10 (1:5000, Abcam), CXCR4 (1:1000, Abcam), stromal cell-derived factor (SDF)-1α (1:1000, Cell Signaling), endothelial nitric oxide synthase (eNOS) (1:1000, Abcam), vascular endothelial cell growth factor (VEGF) (1:1000, Abcam), brain natriuretic peptide (BNP) (1:600, Abcam), myosin heavy chain (MHC)-α (1:300, Santa Cruz), MHC-β (1:1000, Santa Cruz), and actin (1: 10000, Chemicon)] for 1 hour at room temperature. Horseradish peroxidase-conjugated anti-rabbit immunoglobulin IgG (1:2000, Cell Signaling) was used as a secondary antibody for one-hour incubation at room temperature. The washing procedure was repeated eight times within one hour. Immunoreactive bands were visualized by enhanced chemiluminescence (ECL; Amersham Biosciences) and exposed to Biomax L film (Kodak). For purposes of quantification, ECL signals were digitized using Labwork software (UVP).

Oxidative stress reaction in LV myocardium

The Oxyblot Oxidized Protein Detection Kit was purchased from Chemicon (S7150). The DNPH derivatization was carried out on 6 μg of protein for 15 minutes according to the manufacturer's instructions. One-dimensional electrophoresis was carried out on 12% SDS/polyacrylamide gel after DNPH derivatization. Proteins were transferred to nitrocellulose membranes which were then incubated in the primary antibody solution (anti-DNP 1:150) for 2 hours, followed by incubation in secondary antibody solution (1:300) for 1 hour at room temperature. The washing procedure was repeated eight times within 40 minutes. Immunoreactive bands were visualized by enhanced chemiluminescence (ECL; Amersham Biosciences) which was then exposed to Biomax L film (Kodak). For quantification, ECL signals were digitized using Labwork software (UVP). For oxyblot protein analysis, a standard control was loaded on each gel.

Immunofluorescent (IF) and immunohistochemical (IHC) staining

In our laboratory room, negative control antibodies were routinely used in IHC and IF staining. In the present study, all immunofluorescent staining were performed with several negative-control examination to exclude auto-fluorescence (background signals) and non-specific signals. Negative control examinations were performed with following condition: first antibody (antigen specific antibody) only, secondary antibody (fluorescent-conjugated antibodies against first antibody from individual

species) only, and secondary antibody followed by non-specific control IgG.

IF staining was performed for the examinations of CD31+, CXCR4+, and SDF-1α+ cells, and troponin-I in LV myocardium using respective primary antibodies based on our recent study [21]. Moreover, IHC staining was performed for examinations of c-Kit and Sca-1 using respective primary antibodies based on our recent study [21]. Irrelevant antibodies were used as controls in the current study.

Vessel density and arterial muscularization in LV infarct area (IA)

IHC staining of small blood vessels was performed with α-SMA (1:400) as primary antibody at room temperature for 1 hour, followed by washing with PBS thrice. Ten minutes after the addition of anti-mouse-HRP conjugated secondary antibody, the tissue sections were washed with PBS thrice. Then 3,3' diaminobenzidine (DAB) (0.7 gm/tablet) (Sigma) was added, followed by washing with PBS thrice after one minute. Finally, hematoxylin was added as a counter-stain for nuclei, followed by washing twice with PBS after one minute. Three heart sections were analyzed in each rat. For quantification, three randomly selected HPFs (200x) were analyzed in each section. The mean number per HPF for each animal was then determined by summation of all numbers divided by 9.

Muscularization of the arterial medial layer (i.e., an index of vascular remodeling) in LV infarct area was defined as a mean thickness of vessel wall greater than 50% of the lumen diameter in a vessel of diameter > 50 μm. Measurement of arteriolar diameter and wall thickness was achieved using the Image-J software (NIH, Maryland, USA).

Histological study of fibrosis area/infarct area

Masson's trichrome staining was used for studying fibrosis of LV myocardium. Three serial sections of LV myocardium were prepared at 4 μm thickness by Cryostat (Leica CM3050S). The integrated area (μm^2) of fibrosis in the slides was calculated using Image Tool 3 (IT3) image analysis software (University of Texas, Health Science Center, San Antonio, UTHSCSA; Image Tool for Windows, Version 3.0, USA). The fibrotic pixels were manually selected in random i.e., after selection of them blindly from a group of sections available, based on the threshold by color. Three selected sections were quantified for each animal. Three randomly selected high-power fields (HPFs) (100 x) were analyzed in each section. After determining the number of pixels in each fibrotic area per HPF, the numbers of pixels obtained from the three HPFs were summed. The procedure was repeated in two other slides for each animal. The mean pixel number per HPF for each animal was then determined by summating all pixel numbers and dividing by 9. The mean the integrated area (μm^2) of fibrosis in LV myocardium per HPF was obtained using a conversion factor of 19.24 (1 μm^2 represented 19.24 pixels).

The method of calculating the integrated area (μm^2) of infarct area in LV myocardium in the tissue sections was identical to that for the integrated area (μm^2) of fibrotic area using Image Tool 3 (IT3) image analysis software.

Statistical analysis

Quantitative data are expressed as means ± SD. Statistical analysis was adequately performed by ANOVA followed by Bonferroni multiple-comparison post hoc test. SAS statistical software for Windows version 8.2 (SAS institute, Cary, NC) was utilized. A probability value < 0.05 was considered statistically significant.

Results

Relevant baseline variables and echocardiographic findings

The final body weight did not differ among the four groups of animals. Additionally, weight of septum + LV myocardium, heart weight, and the ratio of heart weight to body weight was similar among the four groups (**Table 1**).

Prior to AMI induction, the baseline echocardiographic data showed no significant difference in left ventricular end-diastolic dimension (LVEDD), left ventricular end-systolic dimension (LVESD), left ventricular end-diastolic volume (LVEDV), left ventricular end-systolic volume (LVESV), and left ventricular ejection fraction (LVEF) among the four groups. However, by 42 days after AMI induction, the LVEDD and LVEDV were significantly lower in sham controls (group

Table 1. Baseline characteristics and transthoraxic echocardiographic results of four groups at baseline and six-week after acute myocardial infarction

Variables	Group 1 (n = 8)	Group 2 (n = 8)	Group 3 (n = 8)	Group 4 (n = 8)	*p*-value*
Final body weight (g)	532 ± 38	525 ± 28	525 ± 24	538 ± 29	0.846
Heart weight (g)	1.49 ± 0.10	1.53 ± 0.15	1.52 ± 0.05	1.49 ± 0.07	0.784
Left ventricle + septum	0.95 ± 0.08	1.02 ± 0.09	1.01 ± 0.06	0.98 ± 0.04	0.323
Ratio of heart weight to body weight	0.0281 ± 0.00029	0.0292 ± 0.00019	0.0290 ± 0.00020	0.0286 ± 0.00023	0.618
Echocardiograph (baseline)					
Thickness of IVS (mm)	1.51 ± 0.17	1.54 ± 0.19	1.46 ± 0.15	1.57 ± 0.21	0.875
Thickness of PW (mm)	1.59 ± 0.28	1.67 ± 0.25	1.65 ± 0.22	1.61 ± 0.23	0.758
LVEDD (mm)	8.02 ± 0.92	7.99 ± 0.61	7.78 ± 0.24	7.83 ± 0.82	0.732
LVESD (mm)	4.78 ± 0.67	4.74 ± 0.94	4.84 ± 0.25	4.51 ± 0.75	0.851
LVEDV (μL)	368.3 ± 87.4	363.7 ± 72.1	325.8 ± 90.1	335.6 ± 73.9	0.810
LVESV (μL)	114.8 ± 44.3	109.5 ± 49.5	125.6 ± 30.7	95.8 ± 35.4	0.664
LVFS (%)	42.81 ± 4.19	42.01 ± 7.33	39.50 ± 2.43	42.01 ± 7.77	0.759
LVEF (%)	71.78 ± 4.56	70.57 ± 2.34	67.67 ± 2.34	70.50 ± 8.36	0.694
Echocardiograph (at end of study period)†					
Thickness of IVS (mm)	1.55 ± 0.17^{a}	0.88 ± 0.66^{b}	1.08 ± 0.11^{c}	1.11 ± 0.07^{c}	< 0.001
Thickness of PW (mm)	1.58 ± 0.25	1.23 ± 0.17	1.44 ± 0.15	1.54 ± 0.51	0.785
LVEDD (mm)	8.21 ± 0.88^{a}	9.29 ± 0.58^{b}	8.79 ± 0.16^{c}	8.51 ± 0.19^{c}	0.005
LVESD (mm)	4.82 ± 0.51^{a}	7.19 ± 0.32^{b}	6.71 ± 0.41^{b,c}	6.27 ± 0.51^{c}	< 0.001
LVEDV (μL)	387.4 ± 81.1^{a}	478.4 ± 49.1^{b}	438.5 ± 80.1^{c}	412.4 ± 53.5^{c}	0.003
LVESV (μL)	119.6 ± 40.3^{a}	273.8 ± 35.3^{b}	248.1 ± 41.3^{b,c}	184.3 ± 43.2^{c}	< 0.001
LVEF (%)	68.6 ± 4.55^{a}	43.5 ± 4.41^{b}	47.9 ± 6.09^{b}	54.9 ± 5.24^{c}	< 0.001

Data are expressed as % or mean ± SD. Group 1 = sham control; Group 2 = acute myocardial infarction (AMI) only; Group 3 = AMI + platelet-rich fibrin (PRF); Group 4 = AMI + PRF + adipose-derived mesenchymal stem cell (ADMSC). IVS = inter-ventricular septum; PW = posterior wall; LVEDD = left ventricular end-diastolic dimension; LVESD = left ventricular end-systolic dimension; LVEDV = left ventricular end-diastolic volume; LVESV = left ventricular end-systolic volume; LVEF = left ventricular ejection fraction. *indicates by one-way ANOVA. Different letters (^{a}, ^{b}, ^{c}) being used for grouping, indicating significant difference (< 0.05) among different groups by Bonferroni multiple-comparison post hoc test. †indicates the echocardiography was performed at day 42 after AMI induction.

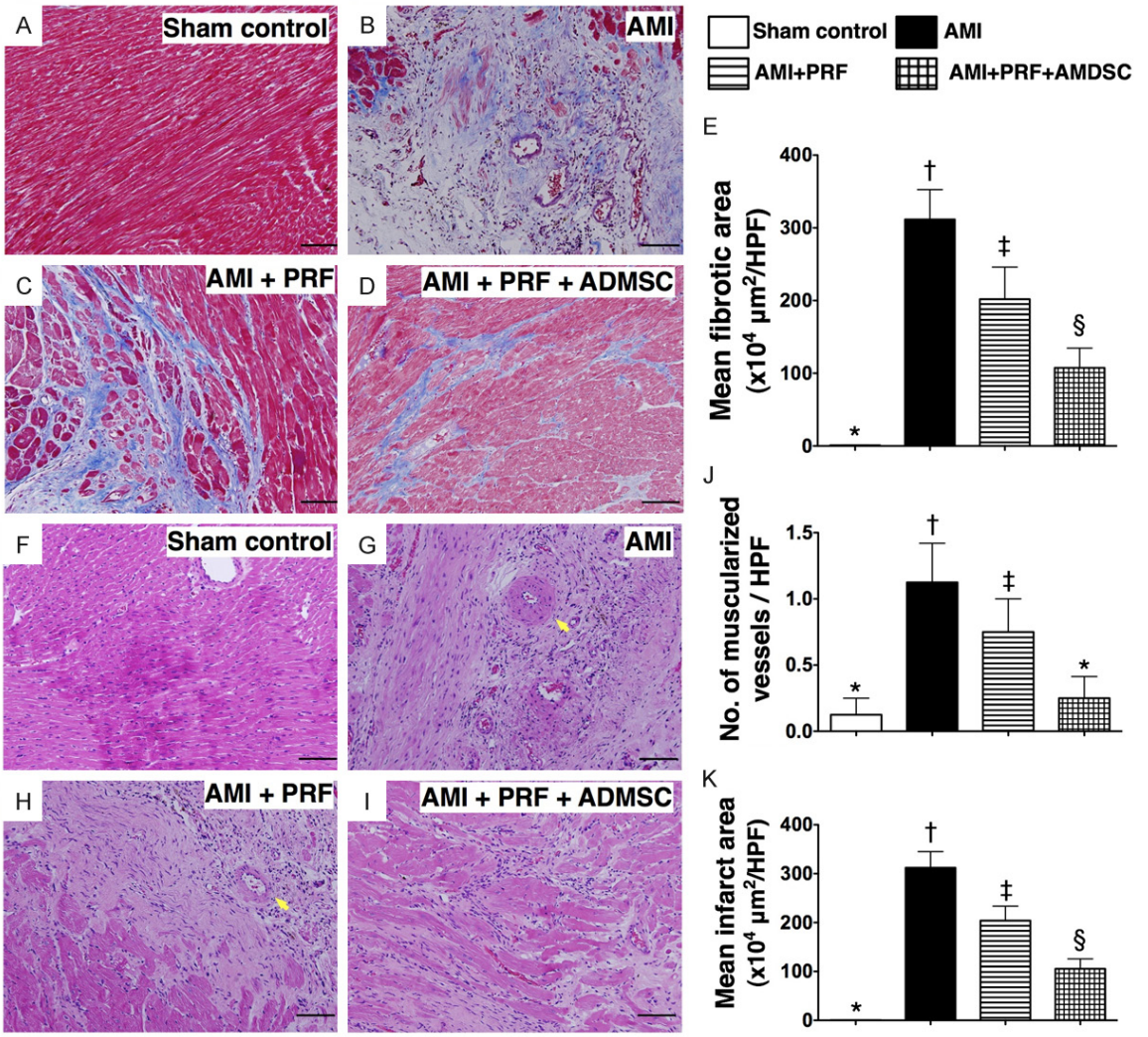

Figure 3. Histopathological findings of LV myocardium on day 42 after AMI induction (n = 8). (A to D) Microscopic findings (100 ×) Masson's Trichrome staining for identifying the fibrotic area in left ventricular (LV) myocardium among four groups. (E) *vs. other groups with different symbols (*, †, ‡, §), $p < 0.0001$. Scale bars in right lower corners represent 100 μm. (F to I) H. & E. staining for identifying the infarct area and number of muscularized vessels in left ventricular (LV) myocardium among four groups. (J) Number of muscularized vessels [yellow arrow in (G) and (H)]: *vs. other groups with different symbols (*, †, ‡), $p < 0.01$. (K) Microscopic findings (100 ×) of infarct area: *vs. other groups with different symbols (*, †, ‡, §), $p < 0.0001$. Scale bars in right lower corners represent 100 μm. HPF = high-power field. Statistical analysis using one-way ANOVA, followed by Bonferroni multiple comparison post hoc test. Symbols (*, †, ‡, §) indicate significance (at 0.05 level).

1) than in AMI only (group 2), AMI + PRF scaffold (group 3) and AMI + PRF scaffold (group 4) animals, but these two parameters did not differ between groups 3 and 4 (**Table 1**). Additionally, the LVESD and LVESV were significantly lower in group 1 than in groups 2, 3 and 4. However, these two parameters only showed tendency of statistically significant difference between groups 2 and 3 ($p = 0.068$) or between groups 3 and 4 ($p = 0.054$). Furthermore, the thickness of inter-ventricular septum was significantly higher in group 1 than in other groups, and significantly higher in groups 3 and 4 than in group 2, but it exhibited no difference between groups 3 and 4. Conversely, the LVEF were significantly lower in groups 2 and 3 than in groups 1 and 4, and notably lower in group 4 than in group 1. However, this parameter only displayed an tendency of statistical significant difference between group 2 and 3 ($p = 0.056$) (**Table 1**). These findings imply that engineered ADMSC grafts treatment provided the most remarkable benefit in preserving LV function and inhibiting LV remodeling.

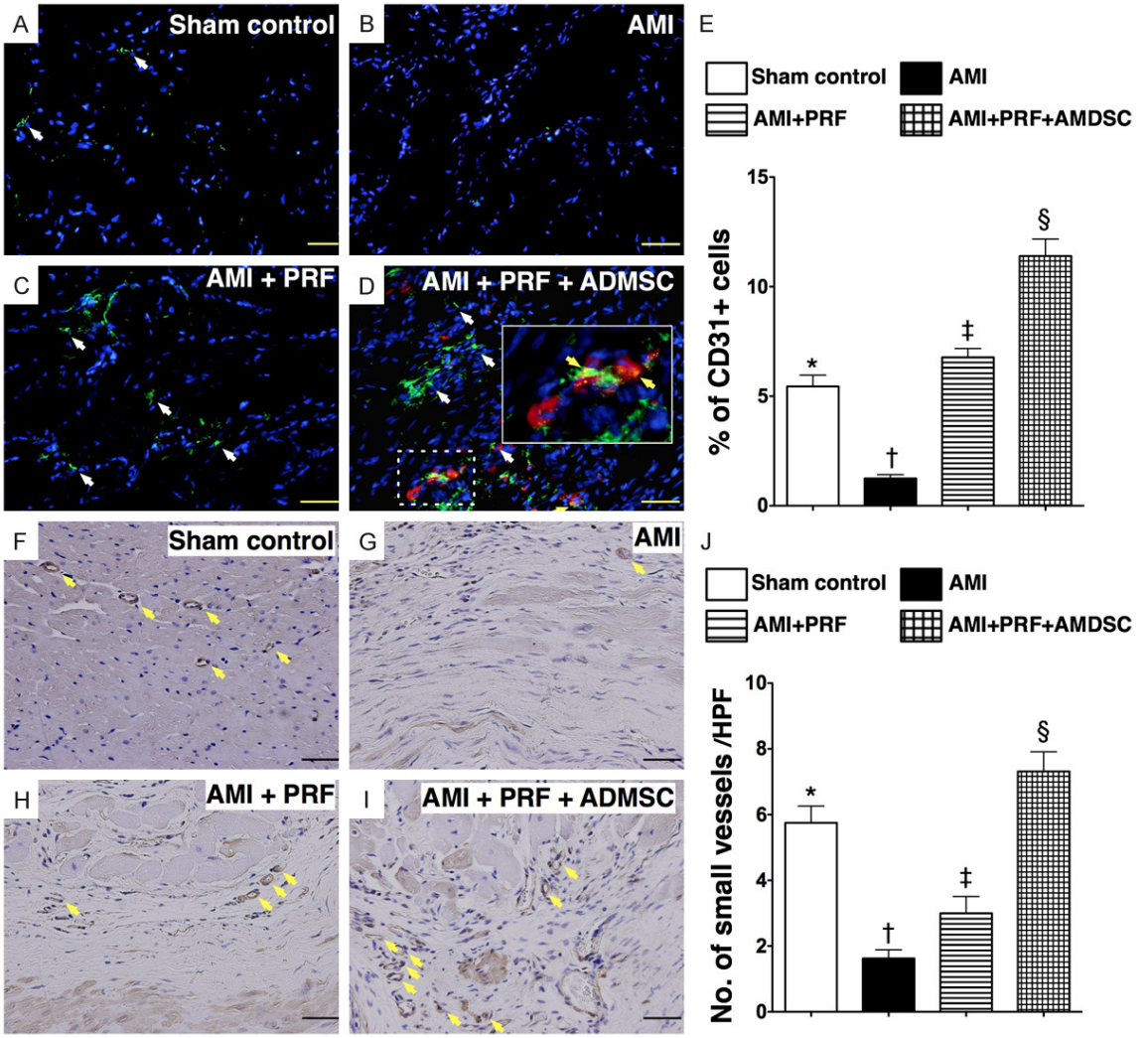

Figure 4. Immunofluorescent (IF) and immunohistochemical (IHC) staining for endothelial cells and small vessels on day 42 after AMI induction (n = 8). (A to D) IF microscopic (200 ×) findings of CD31+ cells (white arrows) in infarct area (IA) of LV myocardium. Red color (D) indicated the DiI-dye stained ADMSCs migrated into the LV myocardium from epicardial engineered ADMSC grafts. Merged image (D) from double staining (DiI-dye + CD31) demonstrating cellular components with mixed red-green color (yellow arrows) under high magnifications (600 ×) (solid-line square from dot-line squared which being magnified), indicating some of engineered ADMSC grafts differentiated into endothelial cells (CD31+). Scale bars in right lower corners represent 50 μm. (E) *vs. other groups with different symbols (*, †, ‡, §), $p < 0.0001$. (F to I) IHC staining (α-smooth muscle actin staining) in infarct area of LV myocardium for identification of small vessels (< 15 μm) (yellow arrows) microscopically (200 ×) in four groups. Scale bars in right lower corners represent 50 μm. (J) *vs. other groups with different symbols (*, †, ‡, §), $p < 0.0001$. HPF = high-power field. Statistical analysis for (E) and (J) using one-way ANOVA, followed by Bonferroni multiple comparison post hoc test. Symbols (*, †, ‡, §) indicate significance (at 0.05 level).

IVISI living imaging, histopathological analysis of left ventricular infarct area

Serial weekly IVIS examinations for 6 weeks showed the persistent presence of near-infrared fluorescence-labeled engineered ADMSC graft on the LV epicardium (**Figure 2A**). This finding indicates that ADMSCs might still survive at the end of the 6-week study period. Additionally, this finding implicates that the biocompatibility and immunogenicity of PRF scaffold is well tolerated by host rat's heart.

The pathological findings identified that the wall thickness was highest in group 1 and lowest in group 2, significantly higher in group 4 than in group 3.

Masson's Trichrome staining demonstrated that the mean fibrotic area was significantly

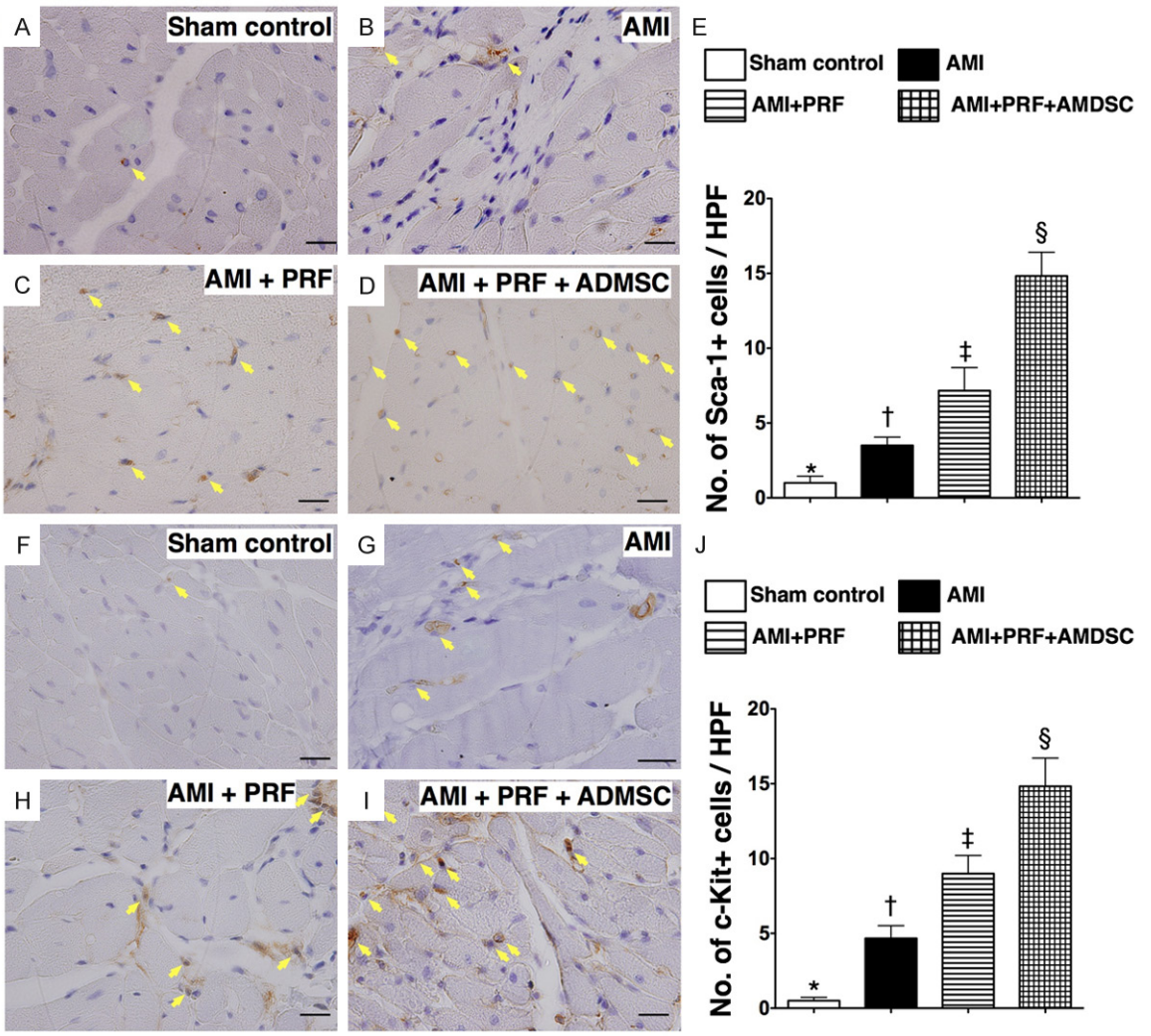

Figure 5. Immunohistochemical (IHC) staining for identification of mesenchymal stem cells in infarct area of LV myocardium on day 42 after AMI induction (n = 8). (A to D) IHC microscopic (200 ×) findings of Sca-1+ cells (yellow arrows) in LV myocardium. (E) *vs. other groups with different symbols (*, †, ‡, §), $p < 0.0001$. (F to I) IHC microscopic (200 ×) findings of c-Kit+ cells (yellow arrows) in LV myocardium. (J) *vs. other groups with different symbols (*, †, ‡, §), $p < 0.0001$. HPF = high-power field. Statistical analysis for (E) and (J) using one-way ANOVA, followed by Bonferroni multiple comparison post hoc test. Symbols (*, †, ‡, §) indicate significance (at 0.05 level).

higher in groups 2 and 3 than in groups 1 and 4, significantly higher in group 2 than in group 3, and significantly higher in group 4 than group 1 (**Figure 3A-E**). In addition, hematoxylin and eosin (H & E) staining (**Figure 3F-I**) showed that the pattern of variation in mean infarct area (IA) was identical to that of fibrotic area among the four groups (**Figure 3K**). Furthermore, the number of muscularized arterioles was notably higher in groups 2 and 3 than in groups 1 and 4, but it showed no difference between groups 2 and 3 or between groups 1 and 4 (**Figure 3J**). These findings indicate that treatment with engineered ADMSC graft was notably better than PRF scaffold per se in attenuating the size of infarct and arterial remodeling after AMI induction.

IHC and IF studies of angiogenesis in infarct area of LV myocardium

The IF staining showed that the number of cells positive for CD31, an indicator of endothelial cell, was highest in group 4 and lowest in group 2, and significantly higher in group 3 than in group 1 (**Figure 4A-E**). Additionally, IHC staining of smooth muscle actin revealed that the number of small vessels (< 15 μm in diameter) in IA,

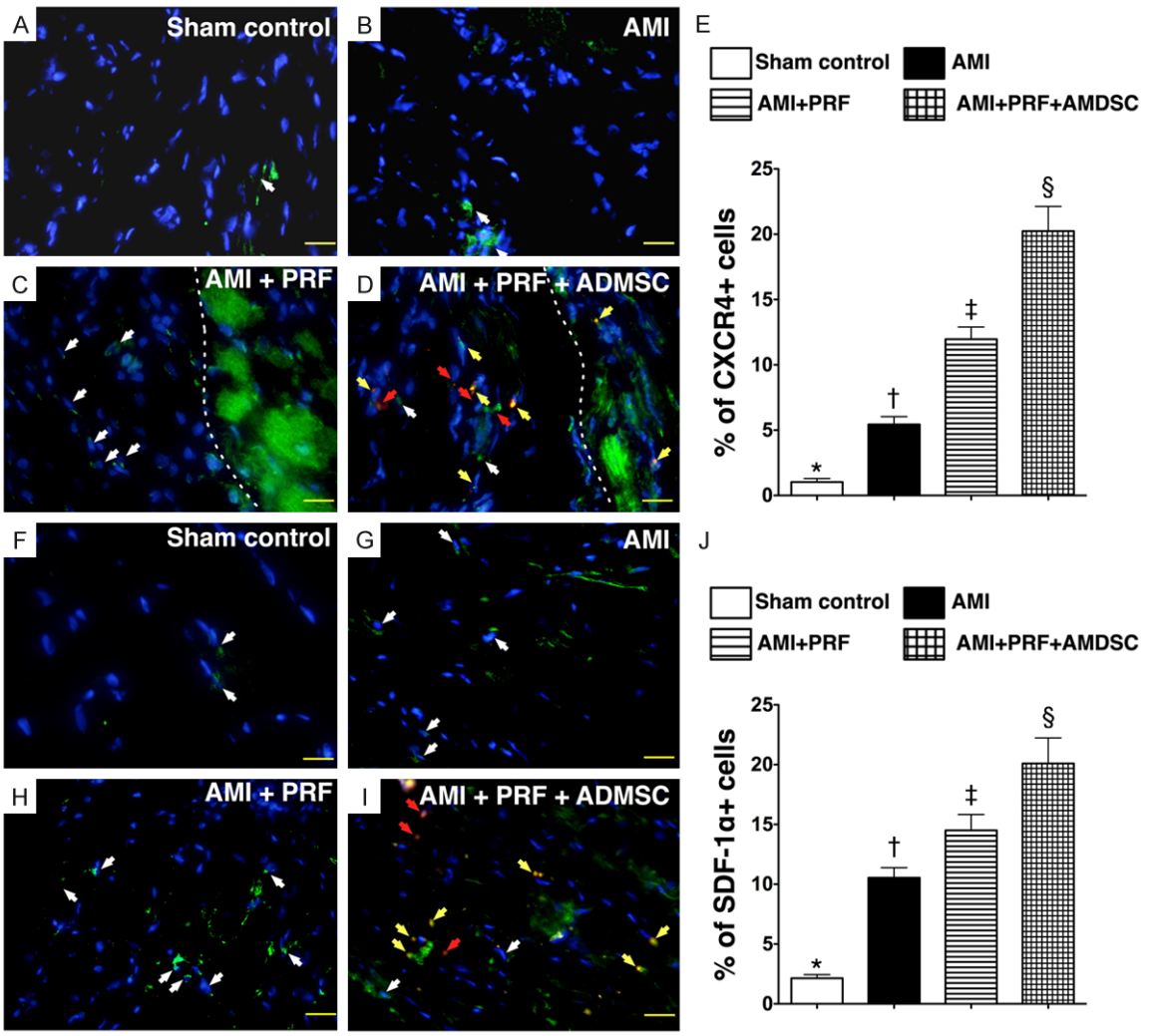

Figure 6. Immunofluorescent (IF) staining for identification of endothelial progenitor cells in infarct area of LV myocardium on day 42 after AMI induction (n = 8). (A to D) IF microscopic (400 ×) findings of CXCR4+ cells (white arrows). Red color in (D) illustration (red arrows) indicated the Dil-dye stained ADMSCs migrated into the LV myocardium from epicardial engineered ADMSC grafts. Merged image (D) from double staining (Dil-dye + CXCR4) demonstrating cellular components with mixed red-green color (yellow arrows), indicating some of engineered ADMSC grafts differentiated into endothelial progenitor cells (EPCs) (CXCR4+). The green color in the right side (separated as left and right side by white dot line) of (C) and (D) illustrations indicted the patched PRF scaffold. Scale bars in right lower corners represent 20 μm. (E) *vs. other groups with different symbols (*, †, ‡, §), $p < 0.0001$. (F to I) IF microscopic (400 ×) findings of SDF-1α+ cells (white arrows) in LV myocardium. Red color in (I) illustration (red arrows) indicated the Dil-dye stained ADMSCs migrated into the LV myocardium from epicardial engineered ADMSC grafts. Merged image (I) from double staining (Dil-dye + SDF-1α) demonstrating cellular components with mixed red-green color (yellow arrows), indicating some of engineered ADMSC grafts differentiated into endothelial EPCs (SDF-1α+). (J) *vs. other groups with different symbols (*, †, ‡, §), $p < 0.0001$. HPF = high-power field. Statistical analysis for (E) and (J) using one-way ANOVA, followed by Bonferroni multiple comparison post hoc test. Symbols (*, †, ‡, §) indicate significance (at 0.05 level).

an index of angiogenesis/neovascularization, was significantly higher in group 4 than in groups 1, 2, and 3, significantly higher in group 1 than in groups 2 and 3, and significantly higher in group 3 than in group 2 (**Figure 4F-J**). This finding suggests that engineered ADMSC graft was superior to RPF scaffold alone in promoting angiogenesis in the IA of LV myocardium.

The IHC staining demonstrated that the numbers of cells positive for Sca-1 (**Figure 5A-E**) and c-Kit (**Figure 5F-J**), two cardiac stem cell markers in the IA, were highest in group 4 and lowest in group 1, and significantly higher in group 3 than in group 2. Furthermore, IF staining showed that the number of cells positive for CXCR4 and SDF-1α, two markers of endothelial

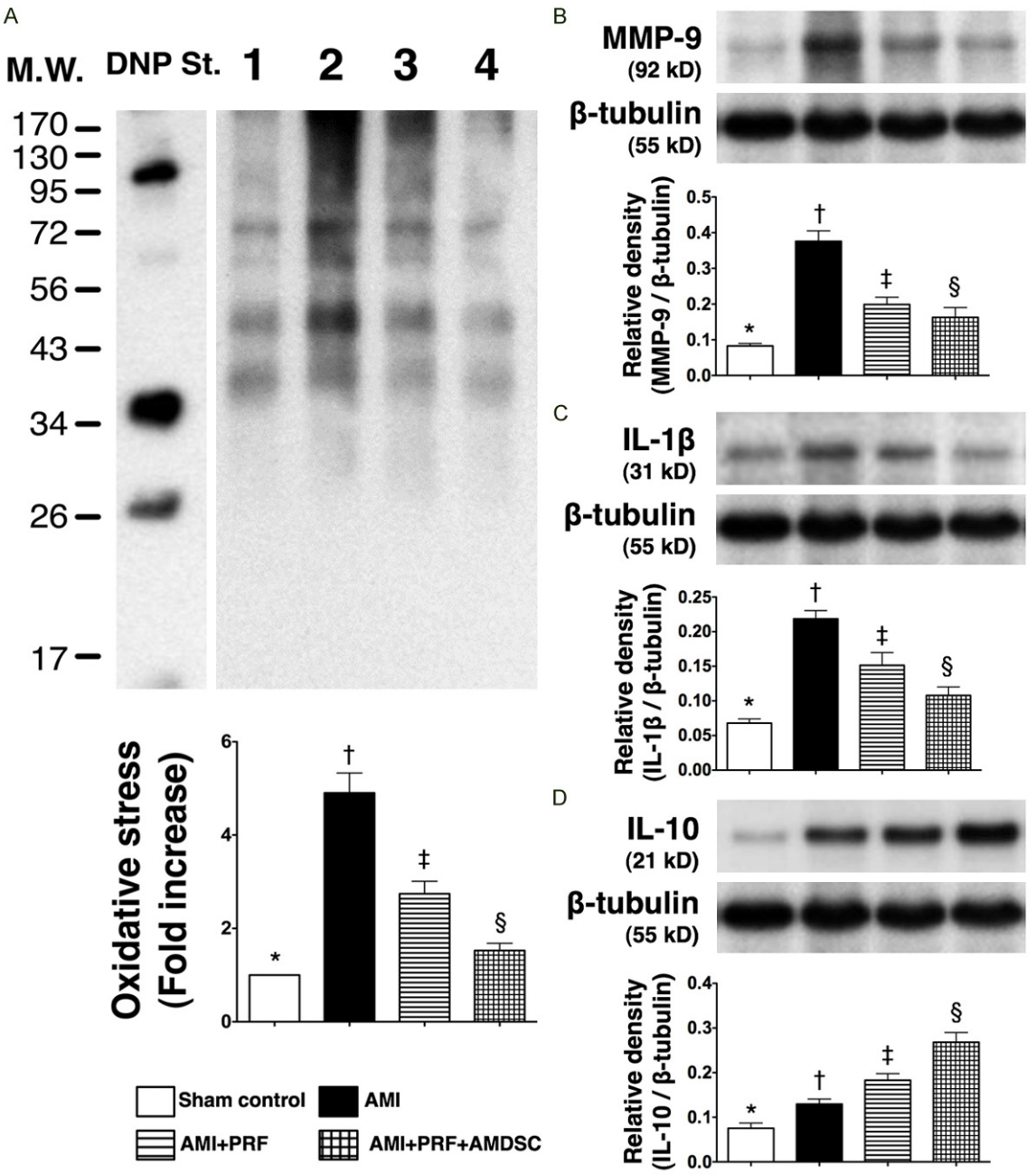

Figure 7. Protein expressions of oxidative stress, inflammation and anti-inflammation in infarct area of LV myocardium on day 42 after AMI induction (n = 8). A. Oxidative index (protein carbonyls) among four groups of animals (1 = sham control, 2 = AMI, 3 = AMI + PRF, 4 = AMI + PRF + ADMSC). Statistical analysis of oxidative stress: *vs. other groups with different symbols (*, †, ‡, §), $p < 0.001$. (Note: Right two lanes shown on the upper panel represent protein molecular weight marker and control oxidized molecular protein standard and, respectively). DNP = 1-3 dinitrophenylhydrazone. W.M. = molecular weight. B. Protein expression of matrix metalloproteinase (MMP)-9. *vs. other groups with different symbols (*, †, ‡, §), $p < 0.001$. C. Protein expression of interleukin (IL)-1β. *vs. other groups with different symbols (*, †, ‡, §), $p < 0.001$. D. Protein expression of IL-10. *vs. other groups with different symbols (*, †, ‡, §), $p < 0.001$. Statistical analysis using one-way ANOVA, followed by Bonferroni multiple comparison post hoc test. Symbols (*, †, ‡, §) indicate significance (at 0.05 level).

progenitor cells (EPCs), were parallel to the number of Sca-1+ and C-kit+ cells in IA among the four groups (**Figure 6**). These findings imply that PRF scaffold *per se* was inferior to engineered ADMSC graft in enhancing angiogenesis in IA. Of importance is that DiI-positive ADMSCs and the cells that were doubly stained (i.e., DiI+ together with CD31, CXCR4, or SDF-

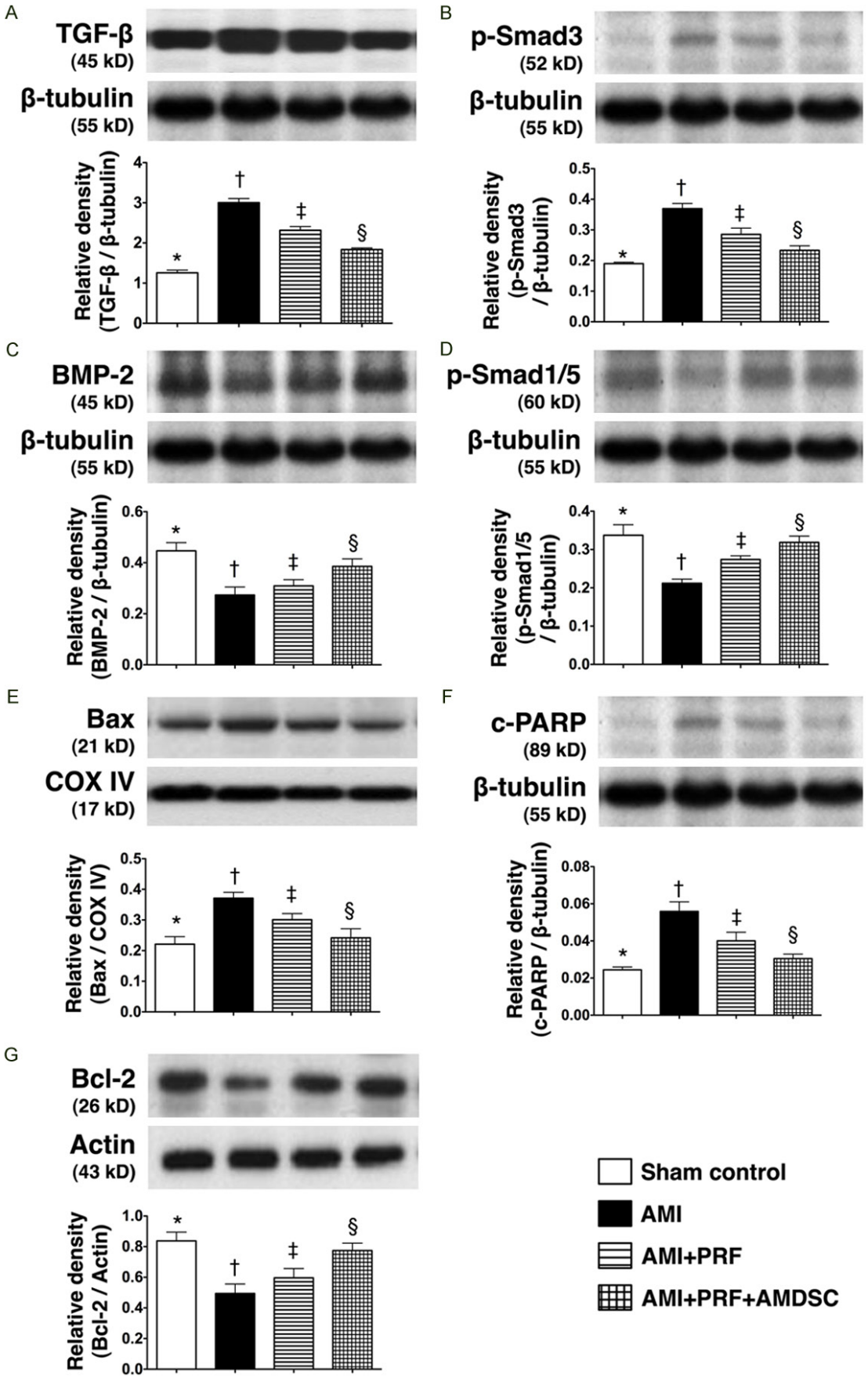
A
TGF-β
(45 kD)
β-tubulin
(55 kD)
Relative density
(TGF-β / β-tubulin)
B
p-Smad3
(52 kD)
β-tubulin
(55 kD)
Relative density
(p-Smad3
/ β-tubulin)
C
BMP-2
(45 kD)
β-tubulin
(55 kD)
Relative density
(BMP-2 / β-tubulin)
D
p-Smad1/5
(60 kD)
β-tubulin
(55 kD)
Relative density
(p-Smad1/5
/ β-tubulin)
E
Bax
(21 kD)
COX IV
(17 kD)
Relative density
(Bax / COX IV)
F
c-PARP
(89 kD)
β-tubulin
(55 kD)
Relative density
(c-PARP / β-tubulin)
G
Bcl-2
(26 kD)
Actin
(43 kD)
Relative density
(Bcl-2 / Actin)
Sham control
AMI
AMI+PRF
AMI+PRF+AMDSC

Figure 8. Protein expressions of fibrotic, anti-fibrotic, apoptotic and anti-apoptotic biomarkers in infarct area of LV myocardium on day 42 after AMI induction (n = 8). A. The protein expression of transforming growth factor (TGF-β). *vs. other groups with different symbols (*, †, ‡, §), $p < 0.001$. B. The protein expression of Smad3. *vs. other groups with different symbols (*, †, ‡, §), $p < 0.01$. C. The protein expression of bone morphogenetic protein (BMP)-2. *vs. other groups with different symbols (*, †, ‡, §), $p < 0.005$. D. The protein expression of Smad1/5. *vs. other groups with different symbols (*, †, ‡, §), $p < 0.01$. E. The protein expression of Bax. *vs. other groups with different symbols (*, †, ‡, §), $p<0.01$. F. The protein expression of cleaved poly(ADP-ribose) polymerase (c-PARP). *vs. other groups with different symbols (*, †, ‡, §), $p < 0.01$. G. The protein expression of Bcl-2. *vs. other groups with different symbols (*, †, ‡, §), $p < 0.01$. Statistical analysis using one-way ANOVA, followed by Bonferroni multiple comparison post hoc test. Symbols (*, †, ‡, §) indicate significance (at 0.05 level).

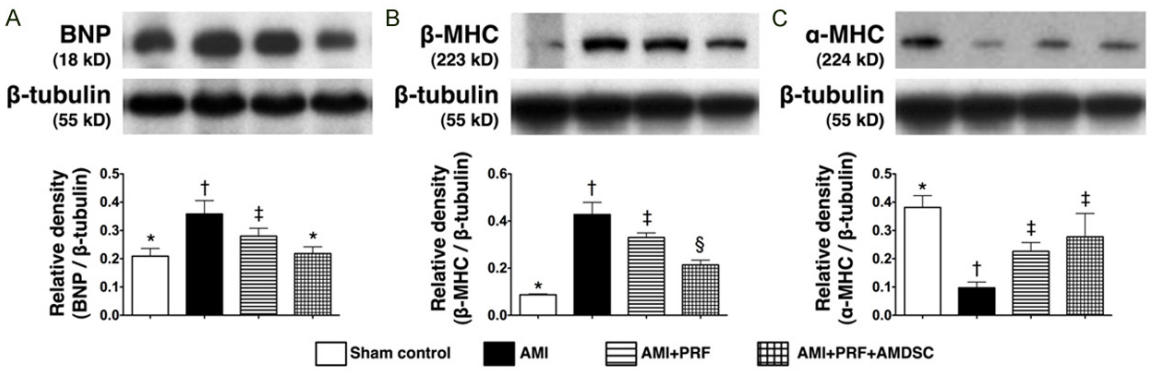

Figure 9. Protein expressions of heart failure and cardiac hypertrophic biomarkers in infarct area of LV myocardium on day 42 after AMI induction (n = 8). A. The protein expression of brain natriuretic peptide (BNP). *vs. other groups with different symbols (*, †, ‡), $p < 0.005$. B. The protein expression of β-myosin heavy chain (MHC). *vs. other groups with different symbols (*, †, ‡, §), $p < 0.008$. C. The protein expression of α-MHC. *vs. other groups with different symbols (*, †, ‡), $p < 0.01$. Statistical analysis using one-way ANOVA, followed by Bonferroni multiple comparison post hoc test. Symbols (*, †, ‡, §) indicate significance (at 0.05 level).

1α positivity indicative of angiogenic cells) were found to be present not only in RPF scaffold but also in LV myocardium (**Figures 4**-**6**). These findings highlight the possibility that these engineered ADMSCs migrated into the myocardium from epicardium and some of them already differentiated into EPCs.

Protein expressions of inflammatory and anti-inflammatory biomarkers in infarct area of left ventricle

The protein expressions of oxidized protein (**Figure 7A**), MMP-9 (**Figure 7B**), IL-1β (**Figure 7C**), three indexes of inflammatory biomarkers, were highest in group 2 and lowest in group 1, and significantly higher in group 3 than in group 4. These findings once more suggest that the biocompatibility and immunogenicity of PRF scaffold is well tolerated by host rat's heart. Conversely, the protein expression of IL-10, an indicator of anti-inflammatory biomarker, showed an opposite pattern compared to that of inflammatory biomarkers among the four groups (**Figure 7D**). These findings suggest that the application of engineered ADMSC graft rather than PRF scaffold contributed to the observed anti-inflammatory activity.

Protein expressions of fibrotic and anti-fibrotic biomarkers in infarct area of left ventricle

The protein expressions of TGF-β and Smad3, two indicators of myocardial fibrosis, were highest in group 2 and lowest in group 1, and significantly higher in group 3 than in group 4 (**Figure 8A** & **8B**). Consistently, the protein expressions of Smad1/5 and BMP-2, two biomarkers of anti-fibrotic activities, exhibited a reversed pattern compared to those of fibrotic biomarkers among the four groups (**Figure 8C** & **8D**). Moreover, the protein expressions of mitochondrial Bax and cleaved (i.e., active form) PARP, two indices of apoptosis, displayed an identical pattern compared to that of fibrotic biomarkers (**Figure 8E** & **8F**). On the other hand, the protein expression of Bcl-2, an index of anti-apoptotic biomarker, showed an opposite pattern compared with that of fibrotic biomarkers among the four groups (**Figure 8G**). These findings sug-

gest that engineered ADMSC graft was superior to PRF scaffold alone in suppressing apoptosis and fibrosis of LV myocardium after AMI.

Protein expressions of heart failure and hypertrophic cardiomyopathic biomarkers in infarct area of left ventricle

The protein expression of BNP, an indicator of heart failure (i.e., due to pressure or volume overload), was highest in group 2 and lowest in group 1, and significantly higher in group 3 than in group 4 (**Figure 9A**). Additionally, since cardiac hypertrophy is characterized by fetal β-MHC gene program activation, a switch of gene expression from α-myosin heavy chain (α-MHC) to β-MHC can serve as a molecular indicator of the severity of cardiac hypertrophy [22, 23]. It was highest in group 2 and lowest in group 1, and significantly higher in group 3 than in group 4 (**Figure 9B**). Accordingly, the protein expression of α-MHC showed an opposite pattern compared with that of β-MHC among the four groups (**Figure 9C**). These findings, therefore, further support that treatment with engineered ADMSC graft rather than PRF scaffold per se attenuated LV remodeling through reducing pressure and/or volume overload after AMI induction.

Protein expressions of angiogenic factors in infarct area of left ventricle

The protein expressions of CXCR4, SDF-1α, and VEGF, three biomarkers of angiogenesis, were lowest in group 1 and highest in group 4, and significantly higher in group 3 than in group 2 (**Figure 10A-C**). In addition, the protein expression of eNOS, an index of endothelial integrity, was highest in group 1 and lowest in group 2, and significantly higher in group 4 than in group 3 (**Figure 10D**). These findings again suggest that engineered ADMSC graft was more effective than PRF scaffold in promoting angiogenesis and preserving endothelial cell function.

Discussion

This study, which assessed the impact of engineered tissue therapy on a rodent model of AMI, provided several striking implications. First, we assessed the effectiveness of PRF scaffold therapy in the enhancement of angiogenesis, preservation of LV function, and suppression of LV remodeling after AMI. Second, our results showed that application of engineered ADMSC graft in the treatment of AMI was superior to PRF scaffold *per se* in augmenting angiogenesis, preserving the thickness of LV wall and LV function, as well as reducing infarct size and LV remodeling. Third, the results of IVIS suggest that PRF scaffold provided a suitable environment for relatively long ADMSC survival.

Despite remarkable advances in pharmacological therapy [3, 8] and reperfusion management strategies [5, 6], LV remodeling after AMI remains an inevitable sequelae [4]. The degree of LV remodeling, which depends on the infarct size and ischemic area [2-4, 8, 9], subsequently determines the increase in LV chamber dimension [3, 4] and wall stress which is directly proportional to the fourth power of chamber radius according to the Laplace's law. The increase in wall stress eventually leads to the loss of cardiomyocytes, thereby resulting in pump failure and unfavorable long-term clinical outcome [3, 4, 8, 9].

Interestingly, some previous clinical studies [24-26] have utilized various surgical approaches to LV reconstruction in an attempt to improve LV contractile function and reduce LV remodeling. Such mechanical support based on the Laplace's law has been reported to provide some favorable clinical benefit for the patients, despite its complicated surgical procedure and risk [27]. One important finding in the present study is that, as compared with AMI animals without treatment, the infarct area (by H & E staining) and the fibrotic area (by Masson's Trichrome staining) were both significantly reduced, whereas the wall thickness in the infarct area was notably preserved in animals receiving PRF scaffold after AMI induction. Additionally, LVEF was also better preserved and LV remodeling was suppressed in AMI animals with than in those without receiving PRF scaffold patching. Our findings are, therefore, comparable to those of clinical trials [26, 27]. The results of the present study, therefore, suggest that patching of PRF scaffold on the infarct LV surface may provide mechanical support that helps in limiting LV dilatation (i.e., a mechanistic basis of according to the Laplace's law) and, therefore, partially preserving cardiac function.

An essential finding in the current study is that the above-mentioned histopathological find-

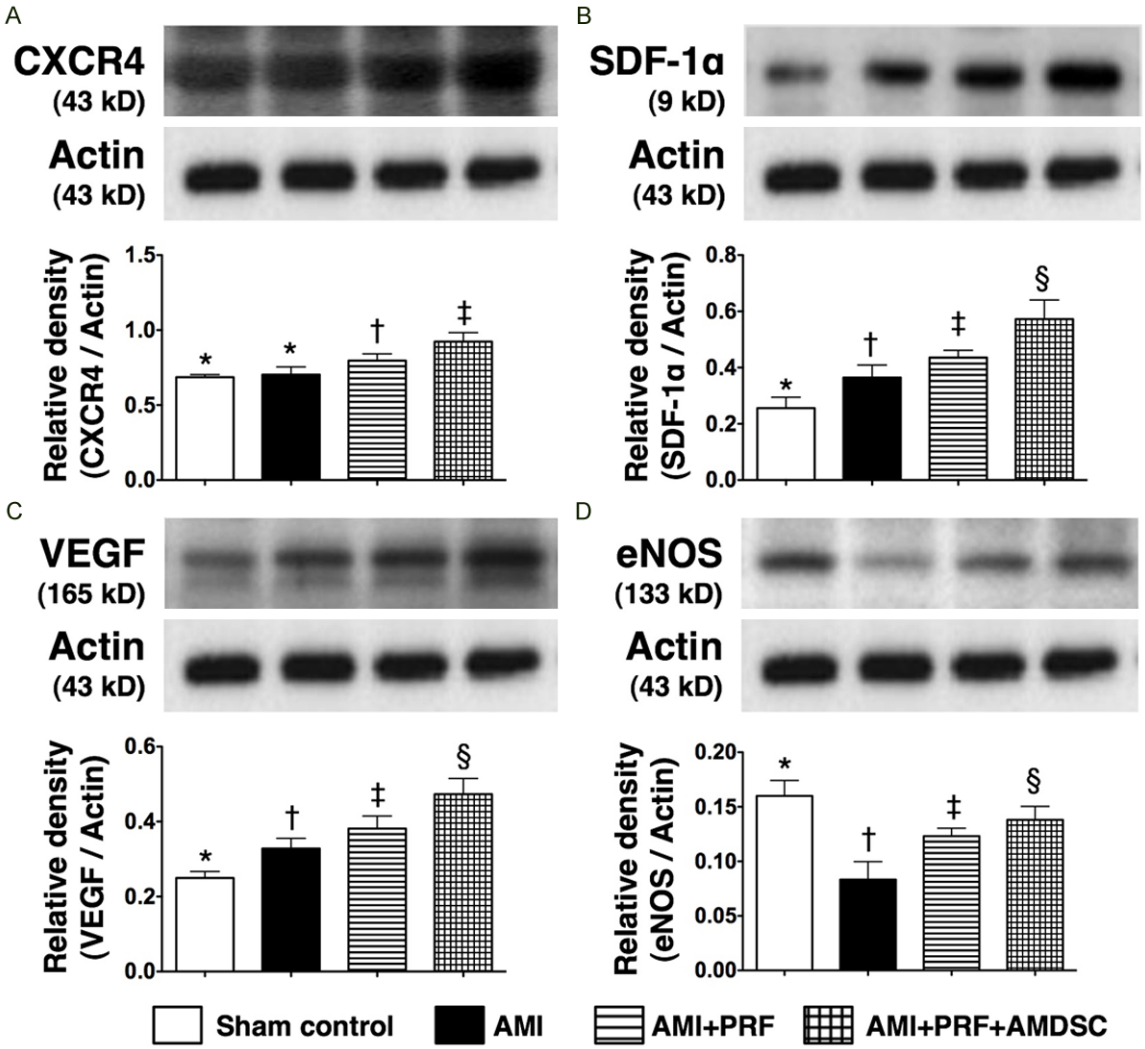

Figure 10. The protein expressions of angiogenetic markers and integrity of endothelial function factors in infarct area of LV myocardium on day 42 after AMI induction (n = 8). A. The protein expression of CXCR4. *vs. other groups with different symbols (*, †, ‡, §), $p < 0.005$. B. The protein expression of stromal cell-derived factor (SDF)-1α. *vs. other groups with different symbols (*, †, ‡, §), $p < 0.004$. C. The protein expression of vascular endothelial growth factor (VEGF). *vs. other groups with different symbols (*, †, ‡, §), $p < 0.005$. D. The protein expression of endothelial nitric oxide synthase (eNOS). *vs. other groups with different symbols (*, †, ‡, §), $p < 0.01$. Statistical analysis using one-way ANOVA, followed by Bonferroni multiple comparison post hoc test. Symbols (*, †, ‡, §) indicate significance (at 0.05 level).

ings, including the infarct and fibrotic areas, were further significantly reduced, whereas the wall thickness in the infarct area was remarkably preserved in animals treated by engineered ADMSC graft than in those receiving PRF scaffold alone. Consistently, as compared with the animals treated by PRF scaffold alone, LVEF was substantially increased, whereas the LV remodeling was notably reduced in those receiving engineered ADMSC graft. Interestingly, experimental studies [28, 29] have recently shown that using stem cells growing on sheet as a confluent monolayer (i.e., cell sheet engineering) to patch on the surface area of infarcted LV myocardium significantly improved heart function. Accordingly, our results strengthen those of studies [28, 29]. On the other hand, the method used in the current study is distinct in several ways. First, the materials used were considerably more economical than those mentioned in recent studies [28, 29]. Second, cell culturing into cell sheets as reported in other studies [28, 29] was not required in the present study that involved minimal *in vitro* manipula-

tion. Third, cell sheets cannot provide the mechanical strength of PRF that was found to suppress LV dilatation in the current study. Fourth, the results of the present study highlight the probability of developing autologous PRF from patients that notably enhances the clinical feasibility of this approach in treating patients with ischemic heart disease or AMI without ethical problem. Finally, the short time of preparing PRF also augments its use in critical conditions such as AMI that mandates immediate intervention.

The mechanisms by which stem cell treatment improves ischemia-related LV dysfunction have been proposed to be multi-faceted, including angiogenesis [13, 16, 17, 30], myogenesis [30, 31], cytokine effects [16], effects of paracrine mediators [31], and myocardial homing by stem cells to the myocardium [32, 33]. In the present study, we found that, as compared with animals with AMI without treatment, the protein expressions of key biomarkers (CXCR4, SDF-1α, eNOS, VEGF) and the number of cells (C-kit+, Sca-1+, CD31+, CXCR4+, SDF-1α+, cells) suggestive of enhanced angiogenesis as well as the number of small vessels indicative of angiogenic activities and neovascularization were significantly increased in the infarct myocardium of animals treated with PRF. Intriguingly, these parameters were further augmented in animals receiving ADMSC-embedded PRF scaffolds. Thus, our findings, in addition to reinforcing the results of previous studies [13, 16, 17, 30], could at least partially explain the improved preservation of LV function using engineered ADMSC grafts.

Abundant data have identified that MSC has typical phenotype of surface markers, including CD90, MSCA-1 (TNAP/W8B2 antigen), CD44, CD29 and CD271+ cells, respectively [34]. Interestingly, the MSC with surface markers of CD90 (the highest population) and CD217, and cardiac stem cell with surface markers of C-kit and Sca-1, were identified In the present study. Therefore, our findings in the present study was comparable with the findings of previous study [34]. Additionally, other recent study has shown that MSCs, including CD29, CD44, and CD73, but not CD31 and CD45 could secrete microvesicles that contain a variety of factors contributing to their angiogenesis-promoting function [35]. In the present study, therapy with ADMSC-embedded PRF scaffolds was found to more enhance angiogenesis than that of PRF therapy alone. In this way, our results reinforced the findings of the recent study [35].

Studies have previously shown that MSCs possess the distinct property of immunomodulation [13, 16, 19, 20]. Moreover, MSC treatment against dilated cardiomyopathy [13], AMI [16], and ischemia-reperfusion injury of other organs [19, 20] significantly reduced the expressions of inflammatory and fibrotic biomarkers and improved ischemia-related organ dysfunction. An interesting finding in the present study is that the protein expressions of inflammatory (oxidized protein, MMP-9, IL-1β) and fibrotic (Smad3, TGF-β) biomarkers, were remarkably decreased in AMI animals with RPF scaffold and further reduced in those receiving engineered ADMSC grafts than in the those without treatment. Conversely, the protein expressions of anti-inflammatory (IL-10) and anti-fibrotic (Smad1/5, BMP-2) biomarkers exhibited a reversed pattern compared to those of inflammatory and fibrotic biomarkers among all groups of animals. Accordingly, our findings, in addition to strengthening those from previous studies [13, 16, 19, 20], could also at least partially explain the significantly improved LV function and suppressed LV remodeling after engineered ADMSC graft treatment.

Up-regulation of β-MHC and down-regulation of α-MHC have been shown to be the specific index of cardiac hypertrophy [22, 23]. Additionally, serum level of BNP has been shown to be a specific biomarker of heart failure and also an important parameter for predicting prognostic outcome after heart failure [36, 37]. Interestingly, our findings demonstrated that the protein expressions of BNP and β-MHC were remarkably higher in AMI animals without treatment as compared with sham controls. These parameters were significantly reduced in AMI animals with PRF scaffolds and further suppressed in AMI animals after receiving engineered ADMSC grafts. On the other hand, the protein expression of α-MHC showed an opposite pattern compared to that of β-MHC among all groups of animals. Our findings, in addition to corroborating those of previous studies [22, 23, 36, 37], once more support the therapeutic potential of engineered ADMSC grafts in reducing LV remodeling in a rodent model of AMI at cellular and molecular levels.

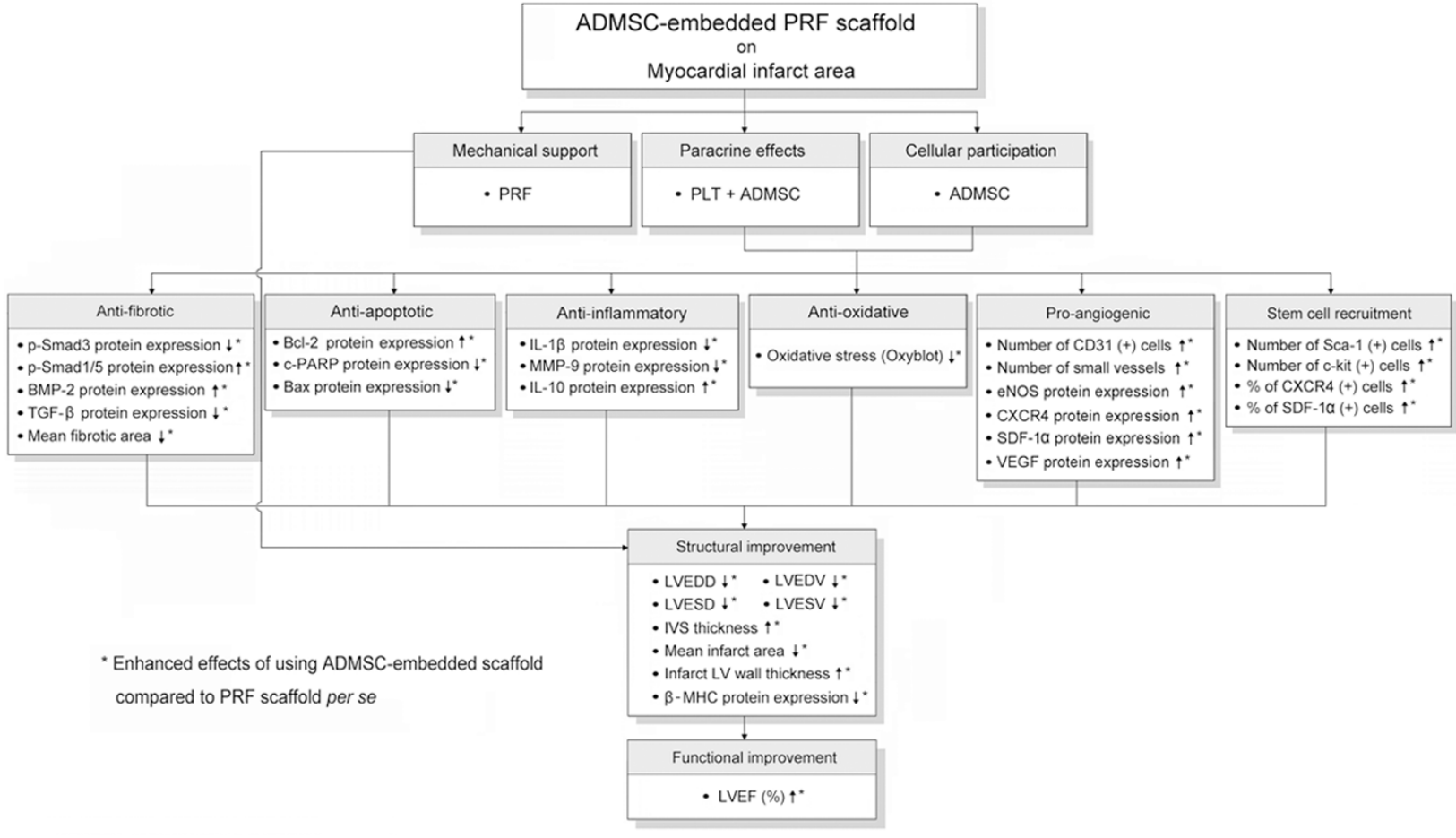

Figure 11. Proposed mechanisms underlying the effects of engineered ADMSC grafts on Improving angiogenesis and heart function and limiting the LV remodeling in a rat AMI model based on findings of the present study. ADMSC = adipose-derived mesenchymal stem cell; PRF = platelet-rich fibrin; BNP = brain natriuretic peptide; TGF = transforming growth factor; c-PARP = cleaved poly(ADP-ribose) polymerase; IL = interleukin; MMP = matrix metalloproteinase; SDF = stromal cell-derived factor; LVEDD = left ventricular end-diastolic dimension; LVEDV = left ventricular end-diastolic volume; VLESD = left ventricular end-systolic dimension; VLESV = left ventricular end-systolic volume; IVS = inter-ventricular septum. MHC = myosin heavy chain; LVEF = left ventricular ejection fraction.

Limitations

This study has limitations. First, the allogeneic rather autologous nature of PRF used in the current study cannot completely exclude the possibility of immune reaction between the graft and the recipient. The use of PRF made from blood of the donor rather than that from the recipient was mainly based on the consideration of high peri-operative morbidity and mortality in the recipients animals after the AMI insult and significant blood withdrawal for PRF synthesis. Second, this study did not utilized the electrocardiogram for identifying AMI in animals and also did not used the triphenyl tetrazolium chloride (TTC) to verify the myocardium infarct size.

Third, the correlation between the scar tissue events and the setting of heart failure did not investigate because practically, it is rather difficult to evaluate the presence or absence of congestive heart failure in rat AMI model. Fourth, this study did not investigate the exactly underlying mechanisms for how the MSC therapy influenced the myocardium and regenerative responses. Additionally, some of the fibrin had been absorbed at the end of the study period. Thus it was too difficult to accurately identify the role of residual fibrin on contribution to the heart weight and volume.

Finally, although extensive work had been done in the current study, the exactly underlying mechanisms involved in the improvement of heart function after engineered ADMSC graft patching has not been fully clarified. The proposed mechanisms have been summarized in **Figure 11** based on our findings.

Conclusion

Compared with treatment with ADMSCs or PRF scaffold alone, patching of the infarcted heart with engineered ADMSC graft in a rodent AMI model offered the most remarkable benefits in enhancing angiogenesis, preserving wall thickness and heart function, as well as reducing infarct size, LV chamber size, and LV remodeling. The findings of this study, therefore, highlight the possibility of future translational application of engineered stem cell graft in the treatment of patients with ischemic heart conditions.

Acknowledgements

This study was supported by a program grant from Chang Gung Memorial Hospital, Chang Gung University (Grant number: CMRPG8A-0561). We thank the molecular imaging core of the Center for Translational Research in Biomedical Sciences, Kaohsiung Chang Gung Memorial Hospital, Kaohsiung, Taiwan for technical and facility supports on IVIS Spectrum and Echo Vevo 2100.

Disclosure of conflict of interest

None.

Address correspondence to: Dr. Hon-Kan Yip, Division of Cardiology, Department of Internal Medicine, Kaohsiung Chang Gung Memorial Hospital, 123, Dapi Road, Niaosung Dist., Kaohsiung City, 83301, Taiwan, R.O.C. Tel: +886-7-7317123; Fax: +886-7-7322402; E-mail: han.gung@msa.hinet.net

References

[1] Murray CJ and Lopez AD. Mortality by cause for eight regions of the world: Global Burden of Disease Study. Lancet 1997; 349: 1269-76.

[2] Erlebacher JA, Weiss JL, Weisfeldt ML and Bulkley BH. Early dilation of the infarcted segment in acute transmural myocardial infarction: role of infarct expansion in acute left ventricular enlargement. J Am Coll Cardiol 1984; 4: 201-8.

[3] Pfeffer MA, Braunwald E, Moyé LA, Basta L, Brown EJ Jr, Cuddy TE, Davis BR, Geltman EM, Goldman S, Flaker GC, et al. Effect of captopril on mortality and morbidity in patients with left ventricular dysfunction after myocardial infarction. Results of the survival and ventricular enlargement trial. The SAVE Investigators. N Engl J Med 1992; 327: 669-77.

[4] Cohn JN, Ferrari R and Sharpe N. Cardiac remodeling--concepts and clinical implications: a consensus paper from an international forum on cardiac remodeling. Behalf of an International Forum on Cardiac Remodeling. J Am Coll Cardiol 2000; 35: 569-82.

[5] The effects of tissue plasminogen activator, streptokinase, or both on coronary-artery patency, ventricular function, and survival after acute myocardial infarction. The GUSTO Angiographic Investigators. N Engl J Med 1993; 329: 1615-22.

[6] Stone GW, Brodie BR, Griffin JJ, Morice MC, Costantini C, St Goar FG, Overlie PA, Popma JJ, McDonnell J, Jones D, O'Neill WW, Grines CL.

Prospective, multicenter study of the safety and feasibility of primary stenting in acute myocardial infarction: in-hospital and 30-day results of the PAMI stent pilot trial. Primary Angioplasty in Myocardial Infarction Stent Pilot Trial Investigators. J Am Coll Cardiol 1998; 31: 23-30.

[7] Yip HK, Chen MC, Chang HW, Hang CL, Hsieh YK, Fang CY, Wu CJ. Angiographic morphologic features of infarct-related arteries and timely reperfusion in acute myocardial infarction: predictors of slow-flow and no-reflow phenomenon. Chest 2002; 122: 1322-32.

[8] Pfeffer MA, Lamas GA, Vaughan DE, Parisi AF and Braunwald E. Effect of captopril on progressive ventricular dilatation after anterior myocardial infarction. N Engl J Med 1988; 319: 80-6.

[9] Mann DL. Mechanisms and models in heart failure: A combinatorial approach. Circulation 1999; 100: 999-1008.

[10] Orlic D, Kajstura J, Chimenti S, Bodine DM, Leri A, Anversa P. Bone marrow cells regenerate infarcted myocardium. Nature 2001; 410: 701-705.

[11] Yang S, Fazel S, Angoulvant D, Weisel RD and Li RK. Cell transplantation for heart disease: the clinical perspective. Evid Based Cardiovasc Med 2005; 9: 2-7.

[12] Nanjundappa A, Raza JA, Dieter RS, Mandapaka S and Cascio WE. Cell transplantation for treatment of left-ventricular dysfunction due to ischemic heart failure: from bench to bedside. Expert Rev Cardiovasc Ther 2007; 5: 125-31.

[13] Yip HK, Chang LT, Wu CJ, Sheu JJ, Youssef AA, Pei SN, Lee FY, Sun CK. Autologous bone marrow-derived mononuclear cell therapy prevents the damage of viable myocardium and improves rat heart function following acute anterior myocardial infarction. Circ J 2008; 72: 1336-45.

[14] Tang XL, Rokosh G, Sanganalmath SK, Yuan F, Sato H, Mu J, Dai S, Li C, Chen N, Peng Y, Dawn B, Hunt G, Leri A, Kajstura J, Tiwari S, Shirk G, Anversa P, Bolli R. Intracoronary administration of cardiac progenitor cells alleviates left ventricular dysfunction in rats with a 30-day-old infarction. Circulation 2010; 121: 293-305.

[15] Zimmet H, Porapakkham P, Porapakkham P, Sata Y, Haas SJ, Itescu S, Forbes A, Krum H. Short- and long-term outcomes of intracoronary and endogenously mobilized bone marrow stem cells in the treatment of ST-segment elevation myocardial infarction: a meta-analysis of randomized control trials. Eur J Heart Fail 2012; 14: 91-105.

[16] Sun CK, Chang LT, Sheu JJ, Chiang CH, Lee FY, Wu CJ, Chua S, Fu M, Yip HK. Bone marrow-derived mononuclear cell therapy alleviates left ventricular remodeling and improves heart function in rat-dilated cardiomyopathy. Crit Care Med 2009; 37: 1197-205.

[17] Simpson D, Liu H, Fan TH, Nerem R, Dudley SC Jr. A tissue engineering approach to progenitor cell delivery results in significant cell engraftment and improved myocardial remodeling. Stem Cells 2007; 25: 2350-7.

[18] Simpson DL, Dudley SC Jr. Modulation of human mesenchymal stem cell function in a three-dimensional matrix promotes attenuation of adverse remodelling after myocardial infarction. J Tissue Eng Regen Med 2013; 7: 192-202.

[19] Leu S, Lin YC, Yuen CM, Yen CH, Kao YH, Sun CK, Yip HK. Adipose-derived mesenchymal stem cells markedly attenuate brain infarct size and improve neurological function in rats. J Transl Med 2010; 8: 63.

[20] Chen YT, Sun CK, Lin YC, Chang LT, Chen YL, Tsai TH, Chung SY, Chua S, Kao YH, Yen CH, Shao PL, Chang KC, Leu S, Yip HK. Adipose-derived mesenchymal stem cell protects kidneys against ischemia-reperfusion injury through suppressing oxidative stress and inflammatory reaction. J Transl Med 2011; 9: 51.

[21] Yeh KH, Sheu JJ, Lin YC, Sun CK, Chang LT, Kao YH, Yen CH, Shao PL, Tsai TH, Chen YL, Chua S, Leu S, Yip HK. Benefit of combined extracorporeal shock wave and bone marrow-derived endothelial progenitor cells in protection against critical limb ischemia in rats. Crit Care Med 2012; 40: 169-77.

[22] Olson EN and Schneider MD. Sizing up the heart: development redux in disease. Genes Dev 2003; 17: 1937-56.

[23] Izumo S, Lompré AM, Matsuoka R, Koren G, Schwartz K, Nadal-Ginard B, Mahdavi V. Myosin heavy chain messenger RNA and protein isoform transitions during cardiac hypertrophy. Interaction between hemodynamic and thyroid hormone-induced signals. J Clin Invest 1987; 79: 970-7.

[24] Lundblad R, Abdelnoor M and Svennevig JL. Repair of left ventricular aneurysm: surgical risk and long-term survival. Ann Thorac Surg 2003; 76: 719-25.

[25] Menicanti L and Di Donato M. Surgical left ventricle reconstruction, pathophysiologic insights, results and expectation from the STICH trial. Eur J Cardiothorac Surg 2004; 26 Suppl 1: S42-6.

[26] Mann DL, Kubo SH, Sabbah HN, Starling RC, Jessup M, Oh JK, Acker MA. Beneficial effects

of the CorCap cardiac support device: five-year results from the Acorn Trial. J Thorac Cardiovasc Surg 2012; 143: 1036-42.

[27] Dor V, Civaia F, Alexandrescu C, Sabatier M and Montiglio F. Favorable effects of left ventricular reconstruction in patients excluded from the Surgical Treatments for Ischemic Heart Failure (STICH) trial. J Thorac Cardiovasc Surg 2011; 141: 905-16, 916, e1-4.

[28] Imanishi Y, Miyagawa S, Maeda N, Fukushima S, Kitagawa-Sakakida S, Daimon T, Hirata A, Shimizu T, Okano T, Shimomura I, Sawa Y. Induced adipocyte cell-sheet ameliorates cardiac dysfunction in a mouse myocardial infarction model: a novel drug delivery system for heart failure. Circulation 2011; 124 Suppl 11: S10-7.

[29] Sekine H, Shimizu T, Dobashi I, Matsuura K, Hagiwara N, Takahashi M, Kobayashi E, Yamato M, Okano T. Cardiac cell sheet transplantation improves damaged heart function via superior cell survival in comparison with dissociated cell injection. Tissue Eng Part A 2011; 17: 2973-80.

[30] Tomita S, Li RK, Weisel RD, Mickle DA, Kim EJ, Sakai T, Jia ZQ. Autologous transplantation of bone marrow cells improves damaged heart function. Circulation 1999; 100 Suppl 19: II247-56.

[31] Mangi AA, Noiseux N, Kong D, He H, Rezvani M, Ingwall JS, Dzau VJ. Mesenchymal stem cells modified with Akt prevent remodeling and restore performance of infarcted hearts. Nat Med 2003; 9: 1195-201.

[32] Jackson KA, Majka SM, Wang H, Pocius J, Hartley CJ, Majesky MW, Entman ML, Michael LH, Hirschi KK, Goodell MA. Regeneration of ischemic cardiac muscle and vascular endothelium by adult stem cells. J Clin Invest 2001; 107: 1395-402.

[33] Quaini F, Urbanek K, Beltrami AP, Finato N, Beltrami CA, Nadal-Ginard B, Kajstura J, Leri A, Anversa P. Chimerism of the transplanted heart. N Engl J Med 2002; 346: 5-15.

[34] Noort WA, Oerlemans MI, Rozemuller H, Feyen D, Jaksani S, Stecher D, Naaijkens B, Martens AC, Bühring HJ, Doevendans PA, Sluijter JP. Human versus porcine mesenchymal stromal cells: phenotype, differentiation potential, immunomodulation and cardiac improvement after transplantation. J Cell Mol Med 2012; 16: 1827-39.

[35] Chen J, Liu Z, Hong MM, Zhang H, Chen C, Xiao M, Wang J, Yao F, Ba M, Liu J, Guo ZK, Zhong J. Proangiogenic compositions of microvesicles derived from human umbilical cord mesenchymal stem cells. PLoS One 2014; 9: e115316.

[36] Kociol RD, Greiner MA, Hammill BG, Eapen ZJ, Fonarow GC, Klaskala W, Mills RM, Curtis LH, Hernandez AF. B-type natriuretic peptide level and postdischarge thrombotic events in older patients hospitalized with heart failure: insights from the Acute Decompensated Heart Failure National Registry. Am Heart J 2012; 163: 994-1001.

[37] Phelan D, Watson C, Martos R, Collier P, Patle A, Donnelly S, Ledwidge M, Baugh J, McDonald K. Modest elevation in BNP in asymptomatic hypertensive patients reflects sub-clinical cardiac remodeling, inflammation and extracellular matrix changes. PLoS One 2012; 7: e49259.